

Okada et al.

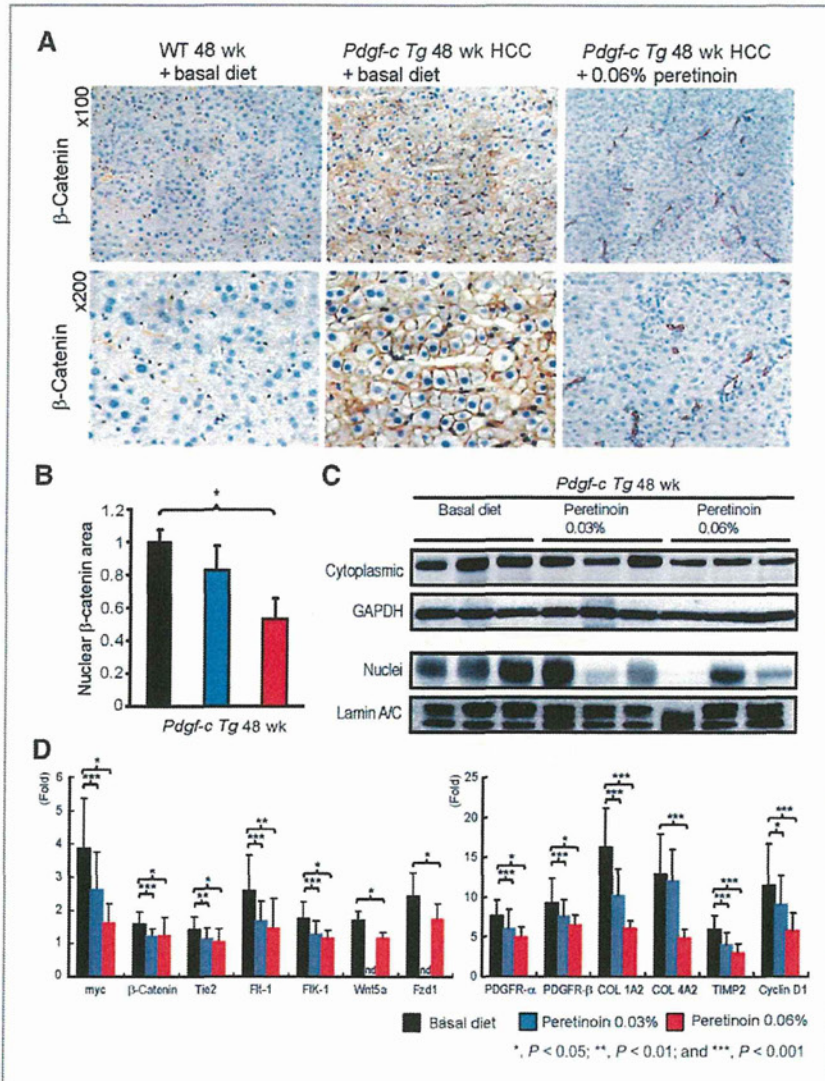


Figure 7. A, IHC staining of  $\beta$ -catenin expression in HCC tissues of *Pdgfr-c Tg* mice fed a basal diet or 0.06% peretinoin at 48 weeks. B, densitometric analysis of  $\beta$ -catenin expression in the liver of *Pdgfr-c Tg* mice fed with different diets ( $n = 15$  for basal diet,  $n = 15$  for 0.03% peretinoin,  $n = 5$  for 0.06% peretinoin). C, Western blotting of  $\beta$ -catenin expression in cytoplasmic and nuclear fractions of *Pdgfr-c Tg* mouse livers fed with different diets. GAPDH was used to standardize cytoplasmic protein and lamin A/C to standardize nuclear protein ( $n = 3$ ). D, RTD-PCR analysis of myc,  $\beta$ -catenin, Tie2, Flt-1, Flk-1, Wnt5a, Fzd1, PDGFR- $\alpha$ , PDGFR- $\beta$ , collagen (COL) 1a2, collagen 4a2, TIMP2, and cyclin D1 expression in HCC tissues of *Pdgfr-c Tg* mice fed with different diets ( $n = 15$  for basal diet,  $n = 15$  for 0.03% peretinoin,  $n = 5$  for 0.06% peretinoin). Relative fold expressions compared with WT mice are shown.

patients with CH-C and HCC to monitor the biological behavior of peretinoin in the liver. Gene expression profiling during peretinoin administration revealed that HCC recurrence within 2 years could be predicted and that PDGF-C expression was one of the strongest predictors. In addition, other genes related to angiogenesis, cancer stem cell and tumor progression were downregulated, whereas expression of genes related to hepatocyte differentiation and tumor suppression was upregulated by peretinoin (data not shown). Moreover, a recent report revealed the emerging significance of PDGF-C-mediated angiogenic and tumorigenic properties (7, 8, 36). In this study, we therefore used the mouse model of *Pdgfr-c Tg*, which displays the phenotypes of hepatic fibrosis, steatosis, and HCC development

that resemble human HCC arising from chronic hepatitis usually associated with advanced hepatic fibrosis.

We showed that peretinoin effectively inhibits the progression of hepatic fibrosis and tumors in *Pdgfr-c Tg* mice (Figs. 1 and 4). Affymetrix gene chips analysis revealed dynamic changes in hepatic gene expression (Supplementary Fig. S3), which were confirmed by IHC staining, RTD-PCR and Western blotting. Pathway analysis of differentially expressed genes suggested that the transcriptional regulators Sp1 and Ap1 are key regulators in the peretinoin inhibition of hepatic fibrosis and tumor development in *Pdgfr-c Tg* mice (Supplementary Fig. S5).

We clearly showed that peretinoin inhibited PDGF signaling through the inhibition of PDGFRs (Figs. 2 and 3). In

addition, we showed that PDGFR repression by peretinoin inhibited primary stellate cell activation (Fig. 5). Interestingly, this inhibitory effect was more pronounced than the effects of 9cRA (Fig. 5B). Normal mouse and human hepatocytes neither express PDGF receptors (J.S. Campbell and N. Fausto, unpublished data), nor proliferate in response to treatment with PDGF ligands (7). However, peretinoin inhibited the expression of PDGFRs, collagens, and their downstream signaling molecules in cell lines of hepatoma (Huh-7, HepG2, and HLE), fibroblast (NIH3T3), endothelial cells (HUVEC), and stellate cells (Lx-2; Supplementary Fig. S6). Furthermore, Sp1 but not Ap1, might be involved in the repression of PDGFR- $\alpha$  in Huh-7 cells (Supplementary Fig. 6C). The over-expression of Sp1-activated PDGFR- $\alpha$  promoter activity, whereas siRNA knockdown of Sp1 repressed PDGFR- $\alpha$  promoter activity in Huh-7 cells (data not shown). Therefore, this seems to confirm that Sp1 is involved in the regulation of PDGFR, as reported previously (37, 38), although these findings should be further investigated in different cell lines. A recent report showed the involvement of transglutaminase 2, caspase3, and Sp1 in peretinoin signaling (35).

Peretinoin was shown to inhibit angiogenesis in the liver of *Pdgfr-c Tg* mice in this study, as shown by the decreased expression of VEGFR1/2 and Tie 2 (Figs. 2 and 6 and Supplementary Fig. S1). Moreover, peretinoin inhibited the number of CD31<sup>+</sup> and CD34<sup>+</sup> endothelial cells (CEC) in the blood and liver (Fig. 6C and D), while also inhibiting the expression of EGFR, c-kit, PDGFRs, and VEGFR1/2 in *Pdgfr-c Tg* mice (data not shown). We also showed that peretinoin inhibited the expression of multiple growth factors such as HGF, IGF, VEGF, PDGF, and HDGF, which were upregulated from 3- to 10-fold in *Pdgfr-c Tg* mice (Supplementary Fig. S3). These activities collectively might contribute to the antitumor effect of peretinoin in *Pdgfr-c Tg* mice. The inhibition of both PDGFRs and VEGFR signaling by peretinoin was previously shown to have a significant effect on tumor growth (36), and we confirmed herein that peretinoin inhibited the expression of VEGFR2 in HUVECs (Supplementary Fig. S6; ref. 39). Finally, we showed that peretinoin inhibited canonical Wnt/ $\beta$ -catenin signaling by showing the decreased nuclear accumulation of  $\beta$ -catenin (Fig. 7). These data confirm the previous hypothesis of transrepression of the  $\beta$ -catenin promoter by 9cRA *in vitro* (40).

Although we showed that the PDGF signaling pathway is a target of peretinoin for preventing the development of hepatic fibrosis and tumors in mice, retinoid-inducing genes such as G0S2 (41), TGM2 (35), CEBPA (42), ATF, TP53BP, metallothionein 1H (MT1H), MT2A, and hemopexin (HPX) were upregulated in peretinoin-treated mice (data not shown). These canonical retinoid pathways are likely to participate in preventing disease progression in conjunction with anti-PDGF effects.

The precise mechanism of peretinoin toxicity, in which 5% of mice treated with 0.06% peretinoin died after 24 weeks of treatment, is currently under investigation. These mice showed severe osteopenia and we speculate that the toxicity might be caused by retinoid-induced osteopenia, as observed in a hypervitaminosis A rat model (43). However, the toxicity of prolonged treatment with oral retinoids in humans remains controversial (44) and severe osteopenia has so far only been seen in a rodent model.

In summary, we show that peretinoin effectively inhibits hepatic fibrosis and HCC development in *Pdgfr-c Tg* mice. Further studies are needed to elucidate the detailed molecular mechanisms of peretinoin action and the effect of peretinoin on PDGF-C in human HCC. The recently developed multi-kinase inhibitor Sorafenib (BAY 43-9006, Nexavar) was shown to improve the prognosis of patients with advanced HCC (45). Promisingly, a phase II/III trial of peretinoin showed it to be safe and well tolerated (46). Therefore, combinatorial therapy that incorporates the use of small molecule inhibitors with peretinoin may be beneficial to some patients. The application of peretinoin during pre- or early-fibrosis stage could be beneficial in preventing the progression of fibrosis and subsequent development of HCC in patients with chronic liver disease.

#### Disclosure of Potential Conflicts of Interest

No potential conflicts of interest were disclosed.

#### Authors' Contributions

**Conception and design:** M. Honda, J.S. Campbell, S. Kaneko  
**Acquisition of data (provided animals, acquired and managed patients, provided facilities, etc.):** H. Okada, M. Honda, J.S. Campbell, Y. Sakai, T. Yamashita, Y. Takebuchi, K. Hada, T. Shirasaki, R. Takabatake, M. Nakamura, H. Sunagozaka, N. Fausto  
**Analysis and interpretation of data (e.g., statistical analysis, biostatistics, computational analysis):** J.S. Campbell, T. Yamashita, H. Sunagozaka, S. Kaneko  
**Writing, review, and/or revision of the manuscript:** H. Okada, M. Honda, J.S. Campbell, N. Fausto, S. Kaneko  
**Study supervision:** J.S. Campbell, S. Kaneko  
**Pathologic examination and evaluation:** T. Tanaka

#### Acknowledgments

The authors thank Dr. Scott Friedman, Mount Sinai School of Medicine (New York, NY), for providing Lx-2 cell lines and Nami Nishiyama and Masayo Baba for their excellent technical assistance.

#### Grant Support

This work was funded by NIH grants CA-23226, CA-174131, and CA-127228 (J.S. Campbell and N. Fausto). This work was also supported in part by a grant-in-aid from the Ministry of Health, Labour and Welfare, and KOWA Co., Ltd., Tokyo, Japan (M. Honda and colleagues).

The costs of publication of this article were defrayed in part by the payment of page charges. This article must therefore be hereby marked *advertisement* in accordance with 18 U.S.C. Section 1734 solely to indicate this fact.

Received January 9, 2012; revised April 27, 2012; accepted May 18, 2012; published OnlineFirst May 31, 2012.

#### References

1. Befeler AS, Di Bisceglie AM. Hepatocellular carcinoma: diagnosis and treatment. *Gastroenterology* 2002;122:1609-19.
2. Mohamed AE, Kew MC, Groenewald HT. Alcohol consumption as a risk factor for hepatocellular carcinoma in urban southern African blacks. *Int J Cancer* 1992;51:537-41.



3. Tsukuma H, Hiyama T, Tanaka S, Nakao M, Yabuuchi T, Kitamura T, et al. Risk factors for hepatocellular carcinoma among patients with chronic liver disease. *N Engl J Med* 1993; 328:1797-801.
4. Deugnier YM, Charalambous P, Le Quilleuc D, Turlin B, Searle J, Brissot P, et al. Preneoplastic significance of hepatic iron-free foci in genetic hemochromatosis: a study of 185 patients. *Hepatology* 1993;18:1363-9.
5. Yeoman AD, Al-Chalabi T, Karani JB, Quaglia A, Devlin J, Mieli-Vergani G, et al. Evaluation of risk factors in the development of hepatocellular carcinoma in autoimmune hepatitis: implications for follow-up and screening. *Hepatology* 2008;48:863-70.
6. Smedile A, Bugianesi E. Steatosis and hepatocellular carcinoma risk. *Eur Rev Med Pharmacol Sci* 2005;9:291-3.
7. Campbell JS, Hughes SD, Gilbertson DG, Palmer TE, Holdren MS, Haran AC, et al. Platelet-derived growth factor C induces liver fibrosis, steatosis, and hepatocellular carcinoma. *Proc Natl Acad Sci U S A* 2005;102:3389-94.
8. Crawford Y, Kasman I, Yu L, Zhong C, Wu X, Modrusan Z, et al. PDGF-C mediates the angiogenic and tumorigenic properties of fibroblasts associated with tumors refractory to anti-VEGF treatment. *Cancer Cell* 2009;15:21-34.
9. Lau DT, Luxon BA, Xiao SY, Beard MR, Lemon SM. Intrahepatic gene expression profiles and alpha-smooth muscle actin patterns in hepatitis C virus induced fibrosis. *Hepatology* 2005;42: 273-81.
10. Honda M, Yamashita T, Ueda T, Takatori H, Nishino R, Kaneko S. Different signaling pathways in the livers of patients with chronic hepatitis B or chronic hepatitis C. *Hepatology* 2006;44: 1122-38.
11. Muto Y, Moriawaki H, Ninomiya M, Adachi S, Saito A, Takasaki KT, et al. Prevention of second primary tumors by an acyclic retinoid, polyphenolic acid, in patients with hepatocellular carcinoma. Hepatoma Prevention Study Group. *N Engl J Med* 1996;334:1561-7.
12. Muto Y, Moriawaki H, Saito A. Prevention of second primary tumors by an acyclic retinoid in patients with hepatocellular carcinoma. *N Engl J Med* 1999;340:1046-7.
13. Suzui M, Masuda M, Lim JT, Albanese C, Pestell RG, Weinstein IB. Growth inhibition of human hepatoma cells by acyclic retinoid is associated with induction of p21(CIP1) and inhibition of expression of cyclin D1. *Cancer Res* 2002;62:3997-4006.
14. Sano T, Kagawa M, Okuno M, Ishibashi N, Hashimoto M, Yamamoto M, et al. Prevention of rat hepatocarcinogenesis by acyclic retinoid is accompanied by reduction in emergence of both TGF- $\alpha$ -expressing oval-like cells and activated hepatic stellate cells. *Nutr Cancer* 2005;51:197-206.
15. Muto Y, Moriawaki H, Omori M. *In vitro* binding affinity of novel synthetic polyphenolics (polyphenolic acids) to cellular retinoid-binding proteins. *Gann* 1981;72:974-7.
16. Yamada Y, Shidoji Y, Fukutomi Y, Ishikawa T, Kaneko T, Nakagawa H, et al. Positive and negative regulations of albumin gene expression by retinoids in human hepatoma cell lines. *Mol Carcinog* 1994;10:151-8.
17. Honda M, Sakai A, Yamashita T, Nakamoto Y, Mizukoshi E, Sakai Y, et al. Hepatic ISG expression is associated with genetic variation in interleukin 28B and the outcome of IFN therapy for chronic hepatitis C. *Gastroenterology* 2010;139:499-509.
18. Frith C, Ward J, Turusov V. Pathology of tumors in laboratory animals. Vol. 2. Lyon, France: IARC Scientific Publications; 1994. p. 223-70.
19. Thoolen B, Maronpot RR, Harada T, Nyska A, Rousseaux C, Nolte T, et al. Proliferative and nonproliferative lesions of the rat and mouse hepatobiliary system. *Toxicol Pathol* 2010;38: 5S-81S.
20. Honda M, Takehana K, Sakai A, Tagata Y, Shirasaki T, Nishitani S, et al. Malnutrition impairs interferon signaling through mTOR and FoxO pathways in patients with chronic hepatitis C. *Gastroenterology* 2011;141:128-40, 140.e1-2.
21. Frith CH, Ward JM, Turusov VS. Tumours of the liver. *IARC Sci Publ* 1994;111:223-69.
22. Xu L, Hui AY, Albanis E, Arthur MJ, O'Byrne SM, Blaner WS, et al. Human hepatic stellate cell lines, LX-1 and LX-2: new tools for analysis of hepatic fibrosis. *Gut* 2005;54:142-51.
23. Nhieu JT, Renard CA, Wei Y, Cherqui D, Zafrani ES, Buendia MA. Nuclear accumulation of mutated beta-catenin in hepatocellular carcinoma is associated with increased cell proliferation. *Am J Pathol* 1999;155:703-10.
24. Wong CM, Fan ST, Ng IO. beta-Catenin mutation and overexpression in hepatocellular carcinoma: clinicopathologic and prognostic significance. *Cancer* 2001;92:136-45.
25. van Zijl F, Mair M, Csiszar A, Schneller D, Zulehner G, Huber H, et al. Hepatic tumor-stroma crosstalk guides epithelial to mesenchymal transition at the tumor edge. *Oncogene* 2009;28: 4022-33.
26. Fischer AN, Fuchs E, Mikula M, Huber H, Beug H, Mikulits W. PDGF essentially links TGF- $\beta$  signaling to nuclear beta-catenin accumulation in hepatocellular carcinoma progression. *Oncogene* 2007;26: 3395-405.
27. Hou X, Kumar A, Lee C, Wang B, Arjunan P, Dong L, et al. PDGF-CC blockade inhibits pathological angiogenesis by acting on multiple cellular and molecular targets. *Proc Natl Acad Sci U S A* 2010;107: 12216-21.
28. Apte U, Zeng G, Muller P, Tan X, Micsenyi A, Cieply B, et al. Activation of Wnt/beta-catenin pathway during hepatocyte growth factor-induced hepatomegaly in mice. *Hepatology* 2006;44:992-1002.
29. Eguchi S, Kanematsu T, Arai S, Omata M, Kudo M, Sakamoto M, et al. Recurrence-free survival more than 10 years after liver resection for hepatocellular carcinoma. *Br J Surg* 2011;98:552-7.
30. Okusaka T, Ueno H, Ikeda M, Morizane C. Phase I and pharmacokinetic clinical trial of oral administration of the acyclic retinoid NIK-333. *Hepatol Res* 2011;41:542-52.
31. Okusaka T, Makuuchi M, Matsui O, Kumada H, Tanaka K, Kaneko S, et al. Clinical benefit of peritoin for the suppression of hepatocellular carcinoma (HCC) recurrence in patients with Child-Pugh grade A (CP-A) and small tumor: a subgroup analysis in a phase II/III randomized, placebo-controlled trial. *J Clin Oncol* 2011;29 Suppl 4s:165.
32. Araki H, Shidoji Y, Yamada Y, Moriawaki H, Muto Y. Retinoid agonist activities of synthetic geranyl geranoic acid derivatives. *Biochem Biophys Res Commun* 1995;209:66-72.
33. Nakamura M, Shidoji Y, Yamada Y, Hatakeyama H, Moriawaki H, Muto Y. Induction of apoptosis by acyclic retinoid in the human hepatoma-derived cell line, HuH-7. *Biochem Biophys Res Commun* 1995;207: 382-8.
34. Yasuda I, Shiratori Y, Adachi S, Obara A, Takemura M, Okuno M, et al. Acyclic retinoid induces partial differentiation, down-regulates telomerase reverse transcriptase mRNA expression and telomerase activity, and induces apoptosis in human hepatoma-derived cell lines. *J Hepatol* 2002;36:660-71.
35. Tatsukawa H, Sano T, Fukaya Y, Ishibashi N, Watanabe M, Okuno M, et al. Dual induction of caspase 3- and transglutaminase-dependent apoptosis by acyclic retinoid in hepatocellular carcinoma cells. *Mol Cancer* 2011;10:4.
36. Timke C, Zieher H, Roth A, Hauser K, Lipson KE, Weber KJ, et al. Combination of vascular endothelial growth factor receptor/platelet-derived growth factor receptor inhibition markedly improves radiation tumor therapy. *Clin Cancer Res* 2008;14: 2210-9.
37. Molander C, Hackzell A, Ohta M, Izumi H, Funa K. Sp1 is a key regulator of the PDGF beta-receptor transcription. *Mol Biol Rep* 2001;28: 223-33.
38. Bonello MR, Khachigian LM. Fibroblast growth factor-2 represses platelet-derived growth factor receptor-alpha (PDGFR- $\alpha$ ) transcription via ERK1/2-dependent Sp1 phosphorylation and an atypical cis-acting element in the proximal PDGFR- $\alpha$  promoter. *J Biol Chem* 2004;279:2377-82.
39. Komi Y, Sogabe Y, Ishibashi N, Sato Y, Moriawaki H, Shimokado K, et al. Acyclic retinoid inhibits angiogenesis by suppressing the MAPK pathway. *Lab Invest* 2010;90:52-60.

40. Shah S, Hecht A, Pestell R, Byers SW. Trans-repression of beta-catenin activity by nuclear receptors. *J Biol Chem* 2003;278:48137-45.
41. Kitareewan S, Blumen S, Sekula D, Bissonnette RP, Lamph WW, Cui Q, et al. G0S2 is an all-trans-retinoic acid target gene. *Int J Oncol* 2008;33:397-404.
42. Uray IP, Shen Q, Seo HS, Kim H, Lamph WW, Bissonnette RP, et al. Retinoid-induced expression of IGFBP-6 requires RARbeta-dependent permissive cooperation of retinoid receptors and AP-1. *J Biol Chem* 2009;284:345-53.
43. Hough S, Avioli LV, Muir H, Gelderblom D, Jenkins G, Kurasi H, et al. Effects of hypervitaminosis A on the bone and mineral metabolism of the rat. *Endocrinology* 1988;122:2933-9.
44. Ribaya-Mercado JD, Blumberg JB. Vitamin A: is it a risk factor for osteoporosis and bone fracture? *Nutr Rev* 2007;65:425-38.
45. Llovet JM, Ricci S, Mazzaferro V, Hilgard P, Gane E, Blanc JF, et al. Sorafenib in advanced hepatocellular carcinoma. *N Engl J Med* 2008;359:378-90.
46. Okita K, Matsui O, Kumada H, Tanaka K, Kaneko S, Moriwaki H, et al. Effect of peretinoin on recurrence of hepatocellular carcinoma (HCC): results of a phase II/III randomized placebo-controlled trial. *J Clin Oncol* 2010;28 Suppl 15s:4024.



## REVIEW

### ***In vitro* models for analysis of the hepatitis C virus life cycle**

Hussein H. Aly<sup>1,2</sup>, Kunitada Shimotohno<sup>3</sup>, Makoto Hijikata<sup>4</sup> and Tsukasa Seya<sup>1</sup>

<sup>1</sup>Department of Microbiology and Immunology, Hokkaido University Graduate School of Medicine, Kita-15, Nishi-7, Kita-ku, <sup>2</sup>Laboratory of Viral Hepatitis and Host Defense, Hokkaido University Creative Research Institution, Kita-22, Nishi-7, Kita-ku, Sapporo 060-8638, <sup>3</sup>Research Institute, Chiba Institute of Technology, Narashino 275-0016, Chiba and <sup>4</sup>Department of Virology, Virus Research Institute, Kyoto University, Kyoto 606-8507, Japan

## ABSTRACT

Chronic hepatitis C virus (HCV) infection affects approximately 170 million people worldwide. HCV infection is a major global health problem as it can be complicated with liver cirrhosis and hepatocellular carcinoma. So far, there is no vaccine available and the non-specific, interferon (IFN)-based treatments now in use have significant side-effects and are frequently ineffective, as only approximately 50% of treated patients with genotypes 1 and 4 demonstrate HCV clearance. The lack of suitable *in vitro* and *in vivo* models for the analysis of HCV infection has hampered elucidation of the HCV life cycle and the development of both protective and therapeutic strategies against HCV infection. The present review focuses on the progress made towards the establishment of such models.

**Key words** hepatitis C virus, HuH-7 cell, knockout mice, type I interferon.

Chronic HCV infection is a major cause of mortality and morbidity throughout the world, infecting approximately 3.1% of the world's population (1). Only a fraction of acutely infected individuals are able to clear the infection spontaneously, whereas approximately 80% of infected individuals develop a chronic infection (2, 3). Patients with chronic HCV are at increased risk for developing liver fibrosis, cirrhosis, and/or hepatocellular carcinoma. Currently, these long-term complications of chronic HCV infection are the leading indication for liver transplantation (4, 5). Because of the high incidence of new infections by blood transfusions in the 1980s before the discovery of the virus, and because morbidity associated with chronic HCV infection generally takes decades to develop, it is expected that the burden of disease in the near future will rise dramatically.

HCV is an enveloped flavivirus, with a positive-stranded RNA genome of approximately 9600 nucleotides. The coding region is flanked by 5' and 3' non-coding regions, which are important for the initiation of translation and regulation of genomic duplication, respectively. The coding region itself is composed of a single open reading frame, which encodes a polyprotein precursor of approximately 3000 amino acids. This polyprotein is cleaved by host and viral proteases into structural and NS proteins (Fig. 1). Replication of the HCV genome involves the synthesis of a full-length negative-stranded RNA intermediate, which in turn provides a template for the de novo production of positive-stranded RNA. Both these synthesis steps are mediated by the viral RNA-dependent RNA polymerase NS5B (6–8). NS5B lacks proofreading abilities, and this leads to a high mutation rate and the

## Correspondence

Hussein H. Aly, Department of Microbiology and Immunology, Graduate School of Medicine, Hokkaido University, Kita-ku, Sapporo 060-8638, Japan.

Tel: +81 11 706 5073; fax: +81 11 706 5056; email: ahussein@med.hokudai.ac.jp

Received 8 September 2011; revised 23 October 2011; accepted 3 November 2011.

**List of Abbreviations:** 3-D, three-dimensional; 3-D/HF, three-dimensional hollow fiber system; bbHCV, blood borne hepatitis C virus; HCV, hepatitis C virus; HPV/E6E7, human papilloma virus E6/E7 genes; IFN, interferon; IFNAR, interferon A receptor; IRES, internal ribosome entry site; ko, knockout; MDA-5, melanoma differentiation associated gene 5; MEF, mouse embryo fibroblasts; mir199, micro RNA 199; NS proteins, non-structural proteins; PPAR, peroxisome proliferator-activated receptor; RFB, radial flow bioreactor; RIG-I, retinoic acid-inducible gene I; TLR, Toll-like receptor; uPA, urokinase plasminogen activator.

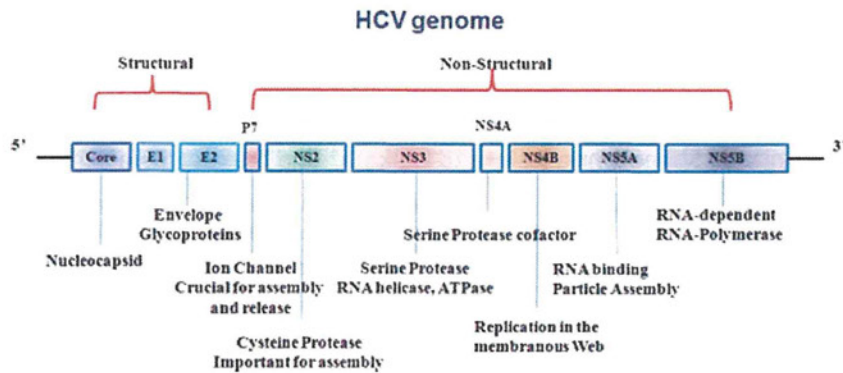


**Fig. 1. Genomic structure of HCV.** Genomic organization of wild-type HCV. The HCV-RNA genome consists of a major open reading frame, encoding a single polyprotein, and an alternative reading frame encoding F-proteins with unknown functions. The cleavage of the polyprotein by viral and host cell proteases gives rise to the mature structural (core, envelope proteins E1 and E2, and p7) and NS viral proteins (NS2 through NS5B). The putative activities and functions of viral proteins are indicated. The IRES located in the 5' non-coding region initiates ribosome binding and translation. Both the 5' and 3' non-coding regions are essential for viral RNA replication involving the RNA-dependent RNA polymerase NS5B. NTPase, nucleotide triphosphatase.

generation of numerous quasispecies. HCV isolates can be classified into seven major genotypes, which vary in sequence by more than 30%. In addition to the distinct prevalence and global spread of the virus, the genotype is an important factor determining disease progression and responses to antiviral therapy (9).

Currently, the only licensed treatment for HCV is the combination of (pegylated)-interferon-alpha (IFN- $\alpha$ ) and ribavirin. Although the success rate of treatment has improved substantially, standard therapy is not effective in all patients. Moreover, severe adverse effects and high costs limit the compliance and global application of this treatment. The development of prophylaxis and novel therapeutics to treat HCV infection has been hampered by the lack of suitable *in vitro* and *in vivo* culture systems. In this review, we describe the development of *in vitro* culture systems for HCV.

### Tissue culture-adapted HCV (sub-)genomic replicons

Dr Bartenschlager's group was the first to establish a convenient reproducible *in vitro* cell culture system for the study of HCV replication (10). They created antibiotic-resistant HCV genomes to select replication-competent viral clones by conveying antibiotic resistance to cells. This was achieved by replacing the structural protein-coding sequences, as well as p7 of the consensus genome Con1, by the neomycin resistance gene. In addition, a second IRES was introduced to promote translation of the non-structural protein-coding sequences important for viral replication (Fig. 2). Upon transfection of these so-called subgenomic replicons in specific cell lines, drug-resistant cell colonies were isolated in which high levels

of viral replication occurred. Subsequent analysis confirmed that these HCV replicons indeed were capable of self-amplification through synthesis of a negative-strand replication intermediate, and could be stably propagated in cell culture for many years (10, 11).

HCV replication was supported by several cell types such as HuH6 (12), HepG2 (13), Li23 (14), and 293 cells (15), with the human hepatoma cell line HuH-7 being the most permissive (16). Interestingly, removal of replicon RNA from these cell clones by treatment with type 1 IFN rendered the cells more permissive to reintroduction of replicons, resulting in higher replication rates. Examples of these highly permissive cells are HuH-7.5 and HuH-7-Lunet cells (16, 17). The efficient replication in the replicon systems was found to depend on tissue-culture-adaptive mutations. Introduction of these specific mutations in the wild-type consensus sequence significantly enhanced viral replication *in vitro* (18–22). Mutational hot spots were found clustered primarily in the NS3, NS4B, and NS5A regions. The mechanisms behind the enhanced replication caused by these tissue-culture-adaptive mutations are still largely unknown, and the interesting fact that these mutations are not commonly found in patients suggests that these may have a toll on the viral fitness.

HCV replicons have proven to be extremely valuable for studies on the process of HCV replication, as well as for testing novel antiviral compounds that specifically target the protease activity of NS3 or the polymerase activity of NS5 (23).

### Cell culture-derived infectious HCV

Studies using HCV replicons have provided detailed knowledge on the mechanisms of replication of HCV.



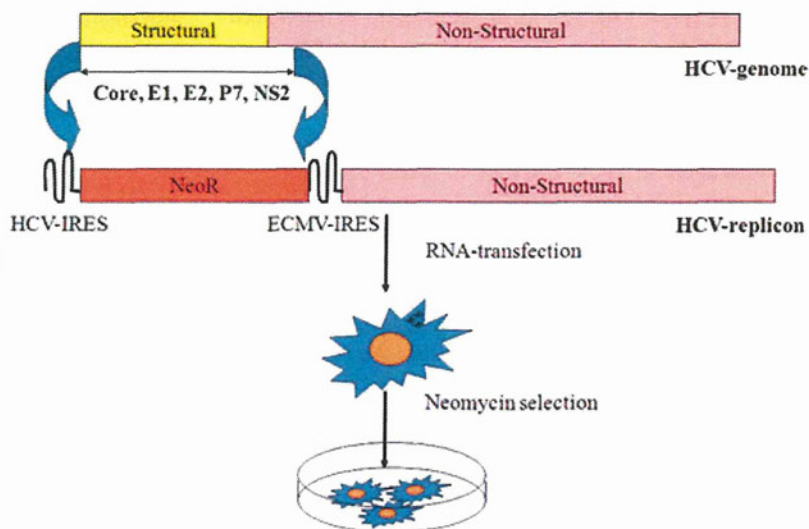


**Fig. 2. HCV replicon system.** The structural sequences (C, E1, E2, and p7) together with NS2 were replaced by a neomycin antibiotic-resistance gene, and an ECMV-IRES was introduced to drive translation of the remaining non-structural proteins. Neomycin selection of these double cistron (bicistronic) replicons in the hepatoma cell line Huh7 resulted in high-level HCV-RNA replication, depending on the gain of so-called 'tissue-culture' adaptive mutations mostly confined to the NS3, NS4B, and NS5A regions.

However, an apparent shortcoming of these models was that stable cell clones containing self-replicating replicons and expressing all viral proteins remained unable to release infectious HCV particles. The inability to secrete viral particles may be the consequence of adaptive mutations, which are needed to enhance viral replication rates, but at the same time may block viral assembly. Indeed, replicons without adaptive mutations show very low replication rates (16, 24). A different situation emerged when the first genotype 2a consensus genome was established (25, 26).

A subgenomic replicon constructed from a clone called JFH-1, isolated from a Japanese patient with fulminant hepatitis C, replicated up to 20-fold higher in HuH-7 cells as compared to Con1 replicons, and did not require adaptive mutations for efficient replication *in vitro* (26). Transfection of HuH-7 and HuH-7.5.1 cells with the

*in vitro*-transcribed full-length JFH-1 genome or a recombinant chimeric genome with another genotype 2a isolate, J6, resulted in the secretion of viral particles that were infectious in cultured cells (Fig. 3), in chimeric mice, and in chimpanzees (27–29).

The infectivity of cells could be neutralized with antibodies against the HCV entry receptor CD81, antibodies against E2, or immunoglobulins from chronically infected patients. Importantly, the replication of cell-cultured HCV in this system was inhibited by IFN- $\alpha$  as well as by several HCV-specific antiviral compounds (29). Since 2005, chimeric JFH-1-based genomes have been constructed of all seven known HCV genotypes. Similar to the J6-JFH-1 chimera, in these so-called intergenotypic recombinants, the structural genes (core, E1, and E2), p7, and NS2 of JFH-1 were replaced by genotype-specific sequences which often resulted in lower infectious virion production than

### Infectious HCV (JFH-1) Production System

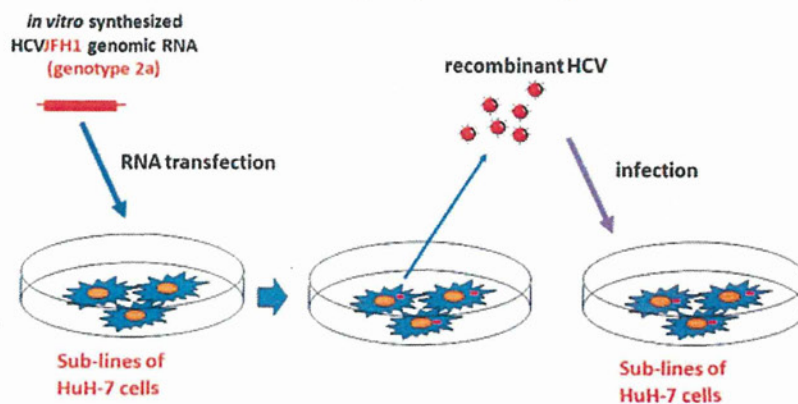


**Fig. 3. JFH1 infectious system.** Full-length JFH1-RNA is transcribed *in vitro*, and transfected to HuH-7-derived cell lines. JFH1 replicates in these cells, and produce infectious virions in the medium. The medium is collected, concentrated, and used to infect naive cells. Hence, the entire HCV life cycle was reproduced for the first time *in vitro*.

wild-type JFH-1 (30–32). Most NS proteins of intergenotypic chimeras originate from JFH-1, and therefore these genomes are unlikely to reflect genotype-specific characteristics of replication. However, these intergenotypic chimeras may become critically important in the study of differences in HCV entry or to assess the efficacy of HCV entry inhibitors. Interestingly, production of infectious genotype 1a HCV in cells transfected with synthetic RNA (H77-S) derived from a prototype virus (H77-C) was also reported (33). H77-S carries adaptive mutations that promote efficient viral RNA replication in HuH-7.5 cells. These mutations are located within the NS3/4A protease complex, and the NS5A protein (34) H77-S showed similar replication efficiency to JFH-1 isolate; however, it showed lower expression of HCV core protein, and lower production of infectious HCV particles (33).

### Serum-derived HCV infection

The previously mentioned models used to study HCV infection are based on subclones of HuH-7 cells infected with JFH1 recombinant virus or its derivatives (27). HuH-7 cells and its subclones, however, do not support the entire life cycle of the bbHCV present in the blood of patients (35). Moreover, HCV has considerable diversity and variability. It is generally classified into six major genotypes and more than 100 subtypes (36). JFH1, however, is a single isolate of HCV genotype 2a that was originally derived from a patient with rare fulminant hepatitis (27). Thus, usage of HCV particles isolated from patient serum could be more useful to study authentic HCV infection.

Many researchers have attempted to develop an *in vitro* system for bbHCV (37–39). These current systems, however, are still insufficient due to their low efficiency for infectivity and replication of bbHCV. Normal human hepatocytes are the ideal system in which to study HCV infectivity. When cultured *in vitro*, however, they proliferate poorly and divide only a few times (40). Continuous proliferation could be achieved by introducing oncogenes, the HPV/E6E7 immortalized multiple cell types that were phenotypically and functionally similar to the parental cells (41–45). We established a human primary non-neoplastic hepatocyte cell line transduced with the HPV18/E6E7 that retained primary hepatocyte characteristics even after prolonged culture (35). We further improved the susceptibility of HPV18/E6E7-immortalized hepatocytes (HuS-E/2 cells) to bbHCV infectivity by impairing the innate immune response of these cells through suppression of interferon regulatory factor-7 (IRF-7) expression. These cells were useful to assay infectivity of HCV strains other than JFH-1, HCV replication, innate immune system engagement of HCV, and screening of anti-HCV agents. This infection system using non-neoplastic cells

also suggested that IRF-7 plays an important role in eliminating HCV infection. Using this system, the suppressive effect of tamoxifen and mir199 on HCV replication was reported (46, 47).

### Three-dimensional culture

A major limitation of the immortalized hepatocytes infection system was the failure to produce infectious HCV particles. Because the 3-D cell culture condition more closely reproduces the *in vivo* environment of hepatocytes (48), culturing these cells in this manner may support the entire HCV life cycle. Similarly, a previous report showed the production of HCV particles from the FLC4 hepatocyte line transfected with HCV-RNA and cultured in a 3-D radial-flow bioreactor (RFB). The RFB system is composed of a dedicated device containing  $1 \times 10^9$  FLC4 cells with a culture area of 2.7 m<sup>2</sup>. A more convenient, smaller and easy to use 3-D culture system is required for the study of the several aspects of bbHCV infection. (49). A hybrid artificial liver support system was developed using animal hepatocytes cultured in a 3-D/HF. This bioartificial liver showed several characteristic features of liver tissue for more than 4 months (50–52).

By growing our HuSE/2 cells in a similar 3-D culture (53) the gene expression profile was improved to more closely match that of human primary hepatocytes. We used this small 3-D culture system and showed it to be ideal for culturing HuS-E/2 cells for the study of bbHCV infection (Fig. 4) (54). Using this system we observed not only the enhancement of HCV replication, but also the production of infectious HCV particles in the medium using the 3-D/HF system. The cell mass formed by the 3-D culture system, most likely the polar character, was essential for the life cycle of bbHCV. Using microarray comparison of gene expression between 2-D and 3-D cultured cells, we found a higher activation of the PPAR- $\alpha$  signaling pathway which was shown to be important for the improvement of HCV replication in 3-D culture. Suppression of the PPAR- $\alpha$  signaling pathway using its antagonist MK886 markedly suppressed HCV replication in two different cell lines (53). A recent study showed that the induction of PPAR- $\alpha$  or PPAR- $\gamma$  led to the suppression or enhancement of HCV replication, respectively, in HuH-7 cells (55). Using HuH-7-derived clones, three different independent studies confirmed our data, showing the suppression of HCV replication by PPAR- $\alpha$  blockers such as (MK886) (56, 57) or 2-chloro-5-nitro-N-(pyridyl) benzamide (BA) (58). Furthermore, no effect of PPAR- $\gamma$  was observed on HCV replication (58).

Delayed production of infectious particles was also observed in cells infected with some HCV strains after prolonged culture (54). It is likely that mutation of the HCV



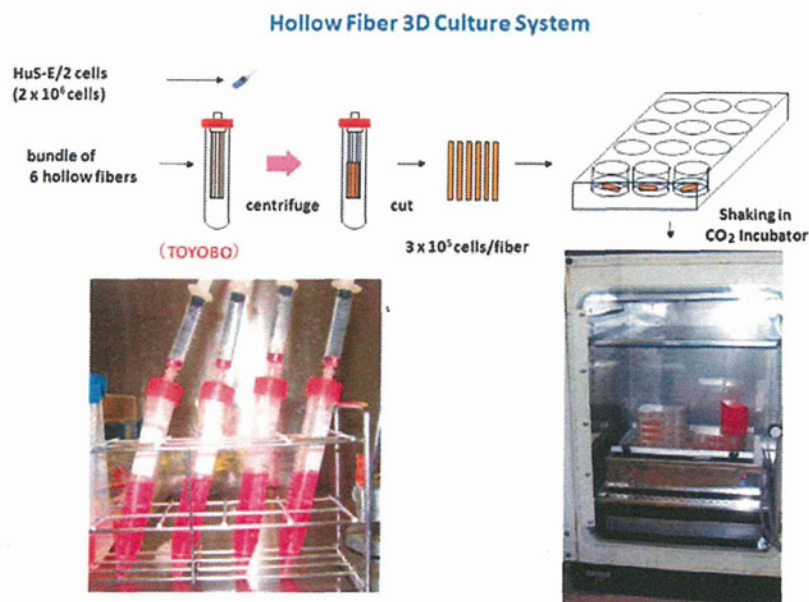


**Fig. 4. 3-D hollow fiber culture.** HuS-E/2 suspension was injected into the lumen of the hollow fiber system (HF; Toyobo Co., Osaka, Japan). The bundles were centrifuged to induce organoid formation. The lower 1.5 cm containing the organoid formation was then cut and cultured in 12-well plates (two capillary bundles per well) with gentle rotation using serum-free medium (Toyobo Co.) in a  $\text{CO}_2$  incubator at  $37^\circ\text{C}$ . The number of cells was adjusted to  $3 \times 10^5$  cells per two-capillary bundle at the start of each experiment.

genome and/or selection of clones during prolonged culture improved the productivity of infectious particles. This lack of production of infectious particles soon after infection may serve to avoid an early strong response from the host immune system, and demonstrates a novel mechanism of latent infection by HCV. Similarly, fluctuation in HCV proliferation was observed during the prolonged culture of 3-D-HuS-E/2 cells infected with bbHCV (54); this fluctuation was associated with a change in viral quasi-species, suggesting that an HCV strain having a growth advantage proliferates selectively and dominantly in these culture conditions. Because the progressive emergence of each dominant strain was only temporary, it is highly likely that the infection and proliferation of such an HCV strain is suppressed by cellular mechanism(s). Our results showed two cellular mechanisms functioning to do this. The first is the involvement of the innate immune system, as evidenced by the secretion of  $\text{IFN-}\alpha$  during the first week of infection. The second mechanism is HCV-induced apoptosis. Although HCV-induced apoptosis was not found when HCV-1b was used for infection, it was found in all cases where HCV-2a was used, suggesting a higher cytopathic tendency of the HCV-2a genotype.

### Mouse cells permissible to HCV infection

The development of prophylaxis and novel therapeutics to treat HCV infection has been hampered by the lack of suitable animal models, a deficit resulting from the limited species tropism of HCV. Chimpanzees are the only available immunocompetent *in vivo* experimental system, but

their use is limited by ethical concerns, restricted availability and prohibitively high costs (59).

A convenient small-animal model supporting the HCV life cycle could significantly accelerate the preclinical testing of vaccine and drug candidates, as well as facilitate *in vivo* studies of HCV pathogenesis. A murine model was described in which overexpression of a uPA transgene resulted not only in neonatal bleeding disorders, but also in severe liver toxicity (60). Importantly, the diseased liver could be replaced by donor hepatocytes of murine origin, as well as by hepatocytes from rats, woodchucks, and humans once the uPA transgenic mice were backcrossed on an immunodeficient background. Mice with chimeric human livers that were inoculated with serum from HCV-positive donors developed prolonged HCV infections with high viral titers and evidence for active replication of the virus in chimeric human livers (61). At present, the chimeric human liver uPA/SCID mouse model is physiologically closest to a natural human infection and therefore represents the most successful small-animal model for HCV infection. Several shortcomings, however, limit its widespread use and application. Most importantly, the immunodeficiency required to allow successful xenotransplantation precludes studies on the adaptive immune response, immunopathology, and active immunization strategies (vaccine development). Second, only a few laboratories have reported successful generation of these chimeras, because this model requires high-quality human donor hepatocytes and the actual transplantation is difficult to carry out in small animals with a tendency to bleed. Finally, the efficacy of human hepatocyte engraftment is highly variable

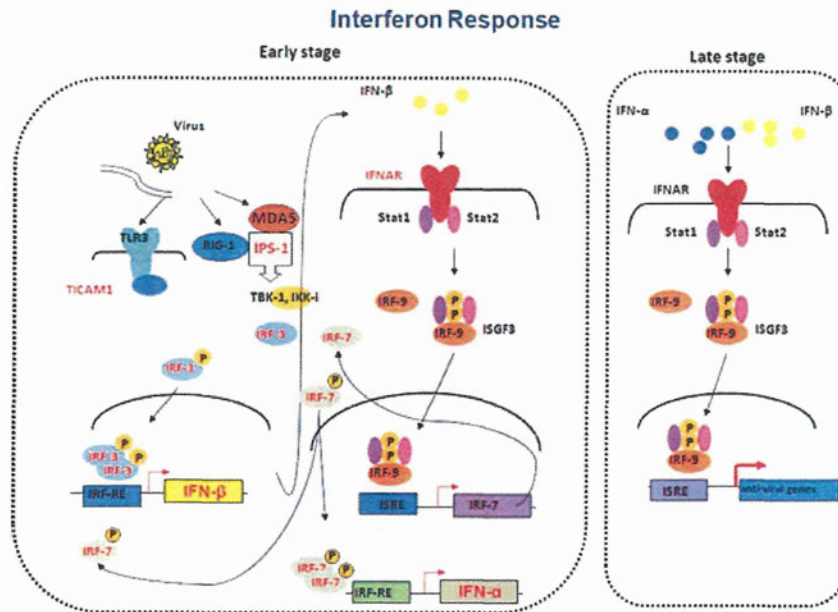


**Fig. 5. Induction of interferon response by viral RNA.** The cell detects viral RNA through the endosomal RNA sensor TLR3, and the cytoplasmic RNA sensors RIG-I and MDA5. Both pathways will lead to the activation of TBK-1 and IKK-ε kinases, through the TICAM-1 adaptor molecule in the case of TLR3, or IPS-1 in the case of RIG-I and MDA5. These kinases will induce phosphorylation of interferon regulatory factor (IRF)-3, which will then dimerize and translocate to the nucleus. IRF-3 will then bind to the IRF response elements (IRF-RE) of IFN-β and lead to the induction of IFN-β expression. The IFN-β that is produced and secreted binds to the IFN receptor in an autocrine or paracrine manner to direct Janus Kinase Signal Transducer and Activator of Transcription (JAK-STAT) signaling and the interferon-stimulated gene factor 3 (ISGF3)-dependent expression of IRF-7 and other interferon-stimulated genes (ISG). IRF-7 will be phosphorylated by the activated TBK-1 and IKK-ε kinases, and form homo, or hetero-dimers with IRF-3, leading to further induction of IFN-β and -α genes. This signaling serves to amplify the IFN response by increasing the expression of IFN-β, IFN-α subtypes and ISG in a positive feedback loop.

in these animals, ranging from approximately 2% to 92% after additional treatment with an antibody to asialo- GM-1 (62).

The successful establishment of the HCV life cycle in mouse hepatocytes is another tempting alternative to overcome these problems. In addition to missing or incompatible positive regulators of HCV replication, dominant-negative restriction factors might be present in mouse hepatocytes. Altered or exacerbated innate antiviral responses, the inability of HCV proteins to overcome murine defenses, or mouse-specific restriction factors similar to those that control retroviral infection, such as Fv1, TRIM5α or APOBEC3 cytidine deaminases, could impair HCV replication in mouse cells.

In mammalian cells, the host detects and responds to infection by RNA-viruses, including HCV, by primarily recognizing viral RNA through several distinct pathogen recognition receptors (PRR), including the cell surface and endosomal RNA sensors TLR3 and TLR7, and the cytoplasmic RNA sensors RIG-I and MDA5 (Fig. 5) (63). The detection of virus infection by these receptors leads to the induction of IFN and their downstream IFN-inducible anti-viral genes through distinct signaling pathways (64).

Type I IFN is an important regulator of viral infections in the innate immune system (65). Another type of IFN, IFN-lambda, affects the prognosis of HCV infection, and its response to antiviral therapy (66,67). Variations in the type or intensity of the antiviral response between hosts are known to restrict the tropism of certain viruses, such as myxoma virus, which is only permissive in mouse cells that have impaired IFN responses. Similarly, we previously reported that the impairment of IRF-7, and suppression of the interferon response improved HCV replication in immortalized primary human hepatocytes. (35)

Mutations impairing the function of the RIG-I gene and the induction of IFN were essential in establishing HCV infectivity in human HuH-7.5 cells (68). Similarly, the HCV-NS3/4a protease is known to cleave the IPS-1 adaptor molecule, inducing further downstream blocking of the IFN-inducing signaling pathway (69). These data clearly demonstrate that the host RIG-I pathway is crucial for suppressing HCV proliferation in human hepatocytes. Using a similar strategy, we investigated whether suppressing the antiviral host innate immune system conferred any advantage on HCV proliferation in mouse hepatocytes (70). We examined the possibility of HCV replication



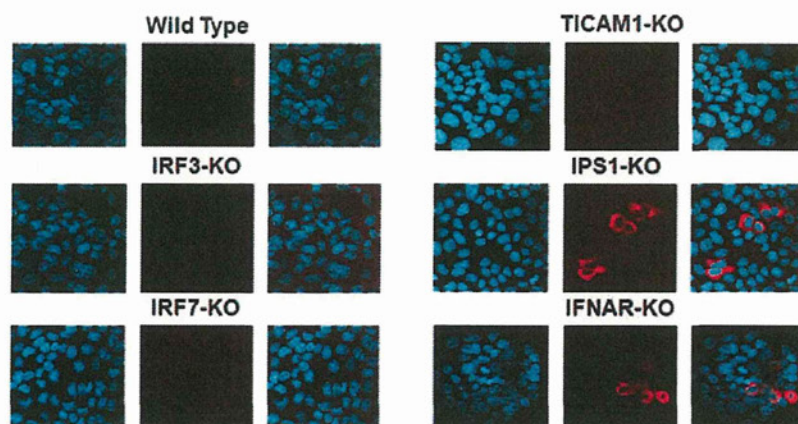


**Fig. 6. Establishment of mouse hepatocyte lines permissive to J6/JFH1.**

Immunofluorescence detection of J6/JFH1 proteins' expression 5 days after transfection of J6/JFH1-RNA through electroporation into wild-type, IRF-3-ko, IRF-7-ko, TICAM1-ko, IPS-1-ko, and IFNAR-ko, freshly isolated primary hepatocytes. A highly sensitive polyclonal antibody extracted from HCV-patient serum (AbS3) was used for the detection.

in mice lacking the expression of key factors that modulate the type I IFN-inducing pathways (Fig. 6). Only gene silencing of IFNAR or IPS-1 was sufficient to establish spontaneous HCV replication in mouse hepatocytes.

To establish a cell line permissive for HCV replication, which is required for further *in vitro* studies of the HCV life cycle in mouse hepatocytes, we immortalized IFNAR- and IPS-1-ko mice hepatocytes with SV40 T antigen. Upon expression of the human (h)CD81 gene, these newly established cell lines were able to support HCV infection and replication for the first time in mouse hepatocytes. Using these cell lines, we demonstrated that the suppression of IPS-1 enhances HCV infection and replication in mouse hepatocytes through the suppression of both IFN induction and an IFN-independent J6/JFH1-induced cytopathic effect. We also showed for the first time the importance of the HCV structural region for viral replication, as JFH1 chimera containing the J6 structure region showed a privilege for spontaneous replication over full-length JFH1 or the subgenomic JFH1 replicon. IRF-3-ko MEF were previously shown to support HCV replication more efficiently than wild MEF (71). As the knockout of IPS-1 mainly suppresses signaling in response to virus RNA detection, and maintains an intact IFN response and induction to other stimulants, it may result in minimum interference to adaptive immune responses as compared to IRF-3 or IFNAR-ko.

## Conclusion

We have established an *in vitro* culture system that can support the entire life cycle of a variety of HCV isolates and genotypes. Although this *in vitro* model system may not completely reproduce the *in vivo* situation, we believe it is the first *in vitro* system showing HCV strain-dependent virus/cell interaction including induction of cellular apoptosis and/or evasion from the cellular innate immune response, which may make it a good tool for the

analysis of virus/host interaction, together with the development of new anti-HCV strategies for the different bbHCV strains. We have also established hepatocyte lines from IPS-1-ko mice that support HCV replication and infection. These cell lines will be very useful in identifying other species' restriction factors and viral determinants required for the further establishment of a robust and efficient HCV life cycle in mouse hepatocytes. Further development of hCD81-transgenic IPS-1-ko mice may serve as a good model for the study of immunological responses against HCV infection. This mouse model can be used as a backbone for any further future models supporting robust HCV infectivity for the study of HCV pathogenesis, propagation and vaccine development.

## ACKNOWLEDGMENT

The author wish to thank Dr. Jin Takahashi from the Japanese NIH, NIID for his help designing figure 5 in this paper.

## DISCLOSURE

The authors declare no financial or commercial conflict of interest.

## REFERENCES

1. Seto W.K., Lai C.L., Fung J., Hung I., Yuen J., Young J., Wong D.K., Yuen M.F. (2010) Natural history of chronic hepatitis C: Genotype 1 versus genotype 6. *J Hepatol.*
2. Conry-Cantilena C., Vanraden M., Gibble J., Melpolder J., Shakil A.O., Viladomiu L., Cheung L., Dibisceglie A., Hoofnagle J., Shih J.W., Kaslow R., Ness P., Alter H.J. (1996) Routes of infection, viremia, and liver disease in blood donors found to have hepatitis C virus infection. *N Engl J Med* 334: 1691–6.
3. Alter M.J., Kruszon-Moran D., Nainan O.V., Mcquillan G.M., Gao F., Moyer L.A., Kaslow R.A., Margolis H.S. (1999) The prevalence of hepatitis C virus infection in the United States, 1988 through 1994. *N Engl J Med* 341: 556–62.
4. Brown R.S. (2005) Hepatitis C and liver transplantation. *Nature* 436: 973–8.

5. Shepard C.W., Finelli L., Alter M.J. (2005) Global epidemiology of hepatitis C virus infection. *Lancet Infect Dis* 5: 558–67.
6. Penin F., Dubuisson J., Rey F.A., Moradpour D., Pawlotsky J.M. (2004) Structural biology of hepatitis C virus. *Hepatology* 39: 5–19.
7. Moradpour D., Penin F., Rice C.M. (2007) Replication of hepatitis C virus. *Nat Rev Microbiol* 5: 453–63.
8. Bartenschlager R., Lohmann V. (2000) Replication of hepatitis C virus. *J Gen Virol* 81: 1631–48.
9. El-Farrash M.A., Aly H.H., Watashi K., Hijikata M., Egawa H., Shimotohno K. (2007) In vitro infection of immortalized primary hepatocytes by HCV genotype 4a and inhibition of virus replication by cyclosporin. *Microbiol Immunol* 51: 127–33.
10. Lohmann V., Korner F., Koch J., Herian U., Theilmann L., Bartenschlager R. (1999) Replication of subgenomic hepatitis C virus RNAs in a hepatoma cell line. *Science* 285: 110–3.
11. Pietschmann T., Lohmann V., Rutter G., Kurpanek K., Bartenschlager R. (2001) Characterization of cell lines carrying self-replicating hepatitis C virus RNAs. *J Virol* 75: 1252–64.
12. Windisch M.P., Frese M., Kaul A., Trippler M., Lohmann V., Bartenschlager R. (2005) Dissecting the interferon-induced inhibition of hepatitis C virus replication by using a novel host cell line. *J Virol* 79: 13778–93.
13. Date T., Kato T., Miyamoto M., Zhao Z., Yasui K., Mizokami M., Wakita T. (2004) Genotype 2a hepatitis C virus subgenomic replicon can replicate in HepG2 and IMY-N9 cells. *J Biol Chem* 279: 22371–6.
14. Kato N., Mori K., Abe K., Dansako H., Kuroki M., Ariumi Y., Wakita T., Ikeda M. (2009) Efficient replication systems for hepatitis C virus using a new human hepatoma cell line. *Virus Res* 146: 41–50.
15. Ali S., Pellerin C., Lamarre D., Kukulj G. (2004) Hepatitis C virus subgenomic replicons in the human embryonic kidney 293 cell line. *J Virol* 78: 491–501.
16. Blight K.J., Mckeating J.A., Rice C.M. (2002) Highly permissive cell lines for subgenomic and genomic hepatitis C virus RNA replication. *J Virol* 76: 13001–14.
17. Friebe P., Boudet J., Simorre J.P., Bartenschlager R. (2005) Kissing-loop interaction in the 3' end of the hepatitis C virus genome essential for RNA replication. *J Virol* 79: 380–92.
18. Lohmann V., Korner F., Dobierzewska A., Bartenschlager R. (2001) Mutations in hepatitis C virus RNAs conferring cell culture adaptation. *J Virol* 75: 1437–49.
19. Lohmann V., Hoffmann S., Herian U., Penin F., Bartenschlager R. (2003) Viral and cellular determinants of hepatitis C virus RNA replication in cell culture. *J Virol* 77: 3007–19.
20. Krieger N., Lohmann V., Bartenschlager R. (2001) Enhancement of hepatitis C virus RNA replication by cell culture-adaptive mutations. *J Virol* 75: 4614–24.
21. Blight K.J., Mckeating J.A., Marcotrigiano J., Rice C.M. (2003) Efficient replication of hepatitis C virus genotype 1a RNAs in cell culture. *J Virol* 77: 3181–90.
22. Blight K.J., Kolykhalov A.A., Rice C.M. (2000) Efficient initiation of HCV RNA replication in cell culture. *Science* 290: 1972–4.
23. Bartenschlager R. (2005) The hepatitis C virus replicon system: from basic research to clinical application. *J Hepatol* 43: 210–6.
24. Pietschmann T., Lohmann V., Kaul A., Krieger N., Rinck G., Rutter G., Strand D., Bartenschlager R. (2002) Persistent and transient replication of full-length hepatitis C virus genomes in cell culture. *J Virol* 76: 4008–21.
25. Kato T., Furusaka A., Miyamoto M., Date T., Yasui K., Hiramoto J., Nagayama K., Tanaka T., Wakita T. (2001) Sequence analysis of hepatitis C virus isolated from a fulminant hepatitis patient. *J Med Virol* 64: 334–9.
26. Kato T., Date T., Miyamoto M., Furusaka A., Tokushige K., Mizokami M., Wakita T. (2003) Efficient replication of the genotype 2a hepatitis C virus subgenomic replicon. *Gastroenterology* 125: 1808–17.
27. Wakita T., Pietschmann T., Kato T., Date T., Miyamoto M., Zhao Z., Murthy K., Habermann A., Krausslich H.G., Mizokami M., Bartenschlager R., Liang T.J. (2005) Production of infectious hepatitis C virus in tissue culture from a cloned viral genome. *Nat Med* 11: 791–6.
28. Zhong J., Gastaminza P., Cheng G., Kapadia S., Kato T., Burton D.R., Wieland S.F., Uprichard S.L., Wakita T., Chisari F.V. (2005) Robust hepatitis C virus infection in vitro. *Proc Natl Acad Sci U S A* 102: 9294–9.
29. Lindenbach B.D., Evans M.J., Syder A.J., Wolk B., Tellinghuisen T.L., Liu C.C., Maruyama T., Hynes R.O., Burton D.R., Mckeating J.A., Rice C.M. (2005) Complete replication of hepatitis C virus in cell culture. *Science* 309: 623–6.
30. Yi M., Ma Y., Yates J., Lemon S.M. (2007) Compensatory mutations in E1, p7, NS2, and NS3 enhance yields of cell culture-infectious intergenotypic chimeric hepatitis C virus. *J Virol* 81: 629–38.
31. Pietschmann T., Kaul A., Koutsoudakis G., Shavinskaya A., Kallis S., Steinmann E., Abid K., Negro F., Dreux M., Cosset F.L., Bartenschlager R. (2006) Construction and characterization of infectious intragenotypic and intergenotypic hepatitis C virus chimeras. *Proc Natl Acad Sci U S A* 103: 7408–13.
32. Gottwein J.M., Scheel T.K., Jensen T.B., Lademann J.B., Prentoe J.C., Knudsen M.L., Hoegh A.M., Bukh J. (2009) Development and characterization of hepatitis C virus genotype 1-7 cell culture systems: role of CD81 and scavenger receptor class B type I and effect of antiviral drugs. *Hepatology* 49: 364–77.
33. Yi M., Villanueva R.A., Thomas D.L., Wakita T., Lemon S.M. (2006) Production of infectious genotype 1a hepatitis C virus (Hutchinson strain) in cultured human hepatoma cells. *Proc Natl Acad Sci U S A* 103: 2310–5.
34. Yi M., Lemon S.M. (2004) Adaptive mutations producing efficient replication of genotype 1a hepatitis C virus RNA in normal Huh7 cells. *J Virol* 78: 7904–15.
35. Aly H.H., Watashi K., Hijikata M., Kaneko H., Takada Y., Egawa H., Uemoto S., Shimotohno K. (2007) Serum-derived hepatitis C virus infectivity in interferon regulatory factor-7-suppressed human primary hepatocytes. *J Hepatol* 46: 26–36.
36. Forns X., Bukh J. (1999) The molecular biology of hepatitis C virus. Genotypes and quasispecies. *Clin Liver Dis* 3: 693–716, vii.
37. Ikeda M., Sugiyama K., Mizutani T., Tanaka T., Tanaka K., Sekihara H., Shimotohno K., Kato N. (1998) Human hepatocyte clonal cell lines that support persistent replication of hepatitis C virus. *Virus Res* 56: 157–67.
38. Chong T.W., Smith R.L., Hughes M.G., Camden J., Rudy C.K., Evans H.L., Sawyer R.G., Pruett T.L. (2006) Primary human hepatocytes in spheroid formation to study hepatitis C infection. *J Surg Res* 130: 52–7.
39. Molina S., Castet V., Pichard-Garcia L., Wychowski C., Meurs E., Pascussi J.M., Sureau C., Fabre J.M., Sacunha A., Larrey D., Dubuisson J., Coste J., Mckeating J., Maurel P., Fournier-Wirth C. (2008) Serum-derived hepatitis C virus infection of primary human hepatocytes is tetraspanin CD81 dependent. *J Virol* 82: 569–74.
40. Delgado J.P., Parouchev A., Allain J.E., Pennarun G., Gauthier L.R., Dutrillaux A.M., Dutrillaux B., Di Santo J., Capron F., Boussin F.D., Weber A. (2005) Long-term controlled immortalization of a primate hepatic progenitor cell line after Simian virus 40 T-Antigen gene transfer. *Oncogene* 24: 541–51.
41. Chen W.H., Lai W.F., Deng W.P., Yang W.K., Lo W.C., Wu C.C., Yang D.M., Lai M.T., Lin C.T., Lin T.W., Yang C.B. (2006) Tissue



- engineered cartilage using human articular chondrocytes immortalized by HPV-16 E6 and E7 genes. *J Biomed Mater Res A* 76: 512–20.
42. Dimri G., Band H., Band V. (2005) Mammary epithelial cell transformation: insights from cell culture and mouse models. *Breast Cancer Res* 7: 171–9.
  43. Harms W., Rothamel T., Miller K., Harste G., Grassmann M., Heim A. (2001) Characterization of human myocardial fibroblasts immortalized by HPV16 E6–E7 genes. *Exp Cell Res* 268: 252–61.
  44. Shiga T., Shirasawa H., Shimizu K., Dezawa M., Masuda Y., Simizu B. (1997) Normal human fibroblasts immortalized by introduction of human papillomavirus type 16 (HPV-16) E6-E7 genes. *Microbiol Immunol* 41: 313–9.
  45. Akimov S.S., Ramezani A., Hawley T.S., Hawley R.G. (2005) Bypass of senescence, immortalization, and transformation of human hematopoietic progenitor cells. *Stem Cells* 23: 1423–33.
  46. Watashi K., Inoue D., Hijikata M., Goto K., Aly H.H., Shimotohno K. (2007) Anti-hepatitis C virus activity of tamoxifen reveals the functional association of estrogen receptor with viral RNA polymerase NS5B. *J Biol Chem* 282: 32765–72.
  47. Murakami Y., Aly H.H., Tajima A., Inoue I., Shimotohno K. (2009) Regulation of the hepatitis C virus genome replication by miR-199a. *J Hepatol* 50: 453–60.
  48. Andrei G. (2006) Three-dimensional culture models for human viral diseases and antiviral drug development. *Antiviral Res* 71: 96–107.
  49. Aizaki H., Nagamori S., Matsuda M., Kawakami H., Hashimoto O., Ishiko H., Kawada M., Matsuura T., Hasumura S., Matsuura Y., Suzuki T., Miyamura T. (2003) Production and release of infectious hepatitis C virus from human liver cell cultures in the three-dimensional radial-flow bioreactor. *Virology* 314: 16–25.
  50. Mizumoto H., Ishihara K., Nakazawa K., Ijima H., Funatsu K., Kajiwara T. (2008) A new culture technique for hepatocyte organoid formation and long-term maintenance of liver-specific functions. *Tissue Eng Part C Methods* 14: 167–75.
  51. Funatsu K., Ijima H., Nakazawa K., Yamashita Y., Shimada M., Sugimachi K. (2001) Hybrid artificial liver using hepatocyte organoid culture. *Artif Organs* 25: 194–200.
  52. Mizumoto H., Aoki K., Nakazawa K., Ijima H., Funatsu K., Kajiwara T. (2008) Hepatic differentiation of embryonic stem cells in HF/organoid culture. *Transplant Proc* 40: 611–3.
  53. Aly H.H., Shimotohno K., Hijikata M. (2009) 3D cultured immortalized human hepatocytes useful to develop drugs for blood-borne HCV. *Biochem Biophys Res Commun* 379: 330–4.
  54. Aly H.H., Qi Y., Atsuzawa K., Usuda N., Takada Y., Mizokami M., Shimotohno K., Hijikata M. (2009) Strain-dependent viral dynamics and virus-cell interactions in a novel in vitro system supporting the life cycle of blood-borne hepatitis C virus. *Hepatology* 50: 689–96.
  55. Nishimura-Sakurai Y., Sakamoto N., Mogushi K., Nagaie S., Nakagawa M., Itsui Y., Tasaka-Fujita M., Onuki-Karakama Y., Suda G., Mishima K., Yamamoto M., Ueyama M., Funaoka Y., Watanabe T., Azuma S., Sekine-Osajima Y., Kakinuma S., Tsuchiya K., Enomoto N., Tanaka H., Watanabe M. (2010) Comparison of HCV-associated gene expression and cell signaling pathways in cells with or without HCV replicon and in replicon-cured cells. *J Gastroenterol* 45: 523–36.
  56. Chockalingam K., Simeon R.L., Rice C.M., Chen Z. (2010) A cell protection screen reveals potent inhibitors of multiple stages of the hepatitis C virus life cycle. *Proc Natl Acad Sci U S A* 107: 3764–9.
  57. Gastaminza P., Whitten-Bauer C., Chisari F.V. (2010) Unbiased probing of the entire hepatitis C virus life cycle identifies clinical compounds that target multiple aspects of the infection. *Proc Natl Acad Sci U S A* 107: 291–6.
  58. Rakic B., Sagan S.M., Noestheden M., Belanger S., Nan X., Evans C.L., Xie X.S., Pezacki J.P. (2006) Peroxisome proliferator-activated receptor alpha antagonism inhibits hepatitis C virus replication. *Chem Biol* 13: 23–30.
  59. Bukh J. (2004) A critical role for the chimpanzee model in the study of hepatitis C. *Hepatology* 39: 1469–75.
  60. Heckel J.L., Sandgren E.P., Degen J.L., Palmiter R.D., Brinster R.L. (1990) Neonatal bleeding in transgenic mice expressing urokinase-type plasminogen activator. *Cell* 62: 447–56.
  61. Mercer D.F., Schiller D.E., Elliott J.F., Douglas D.N., Hao C., Rinfret A., Addison W.R., Fischer K.P., Churchill T.A., Lakey J.R., Tyrrell D.L., Kneteman N.M. (2001) Hepatitis C virus replication in mice with chimeric human livers. *Nat Med* 7: 927–33.
  62. Tateno C., Yoshizane Y., Saito N., Kataoka M., Utoh R., Yamasaki C., Tachibana A., Soeno Y., Asahina K., Hino H., Asahara T., Yokoi T., Furukawa T., Yoshizato K. (2004) Near completely humanized liver in mice shows human-type metabolic responses to drugs. *Am J Pathol* 165: 901–12.
  63. Diamond M.S. (2009) Mechanisms of evasion of the type I interferon antiviral response by flaviviruses. *J Interferon Cytokine Res* 29: 521–30.
  64. O'Neill L.A., Bowie A.G. (2010) Sensing and signaling in antiviral innate immunity. *Curr Biol* 20: R328–33.
  65. Platanias L.C. (2005) Mechanisms of type-I- and type-II-interferon-mediated signalling. *Nat Rev Immunol* 5: 375–86.
  66. Tanaka Y., Nishida N., Sugiyama M., Kurosaki M., Matsuura K., Sakamoto N., Nakagawa M., Korenaga M., Hino K., Hige S., Ito Y., Mita E., Tanaka E., Mochida S., Murawaki Y., Honda M., Sakai A., Hiasa Y., Nishiguchi S., Koike A., Sakaida I., Imamura M., Ito K., Yano K., Masaki N., Sugauchi F., Izumi N., Tokunaga K., Mizokami M. (2009) Genome-wide association of IL28B with response to pegylated interferon-alpha and ribavirin therapy for chronic hepatitis C. *Nat Genet* 41: 1105–9.
  67. Thompson A.J., Muir A.J., Sulkowski M.S., Ge D., Fellay J., Shianna K.V., Urban T., Afdhal N.H., Jacobson I.M., Esteban R., Poordad F., Lawitz E.J., Mccone J., Shiffman M.L., Galler G.W., Lee W.M., Reindollar R., King J.W., Kwo P.Y., Ghalib R.H., Freilich B., Nyberg L.M., Zeuzem S., Poynard T., Vock D.M., Pieper K.S., Patel K., Tillmann H.L., Noviello S., Koury K., Pedicone L.D., Brass C.A., Albrecht J.K., Goldstein D.B., Mchutchison J.G. (2010) Interleukin-28B polymorphism improves viral kinetics and is the strongest pretreatment predictor of sustained virologic response in genotype 1 hepatitis C virus. *Gastroenterology* 139: 120–9 e18.
  68. Sumpter R., Jr., Loo Y.M., Foy E., Li K., Yoneyama M., Fujita T., Lemon S.M., Gale M., Jr. (2005) Regulating intracellular antiviral defense and permissiveness to hepatitis C virus RNA replication through a cellular RNA helicase, RIG-I. *J Virol* 79: 2689–99.
  69. Foy E., Li K., Sumpter R., Jr., Loo Y.M., Johnson C.L., Wang C., Fish P.M., Yoneyama M., Fujita T., Lemon S.M., Gale M., Jr. (2005) Control of antiviral defenses through hepatitis C virus disruption of retinoic acid-inducible gene-I signaling. *Proc Natl Acad Sci U S A* 102: 2986–91.
  70. Aly H.H., Oshiumi H., Shime H., Matsumoto M., Wakita T., Shimotohno K., Seya T. (2011) Development of mouse hepatocyte lines permissive for hepatitis C virus (HCV). *PLoS One* 6: e21284.
  71. Lin L.T., Noyce R.S., Pham T.N., Wilson J.A., Sisson G.R., Michalak T.I., Mossman K.L., Richardson C.D. (2010) Replication of subgenomic hepatitis C virus replicons in mouse fibroblasts is facilitated by deletion of interferon regulatory factor 3 and expression of liver-specific microRNA 122. *J Virol* 84: 9170–80.

## ORIGINAL ARTICLE

# Regulation of immunological balance by sustained interferon- $\gamma$ gene transfer for acute phase of atopic dermatitis in mice

K Watcharanurak<sup>1</sup>, M Nishikawa<sup>1</sup>, Y Takahashi<sup>1</sup>, K Kabashima<sup>2</sup>, R Takahashi<sup>3</sup> and Y Takakura<sup>1</sup>

Interferon (IFN)- $\gamma$ , a potent T helper 1 (Th1) cell cytokine, is suggested to suppress Th2 cell responses. Here, we aimed to investigate whether pCpG-Mu $\gamma$ , a plasmid continuously expressing murine IFN- $\gamma$ , is an effective treatment of atopic dermatitis, a Th2-dominant skin disease. Nishiki-nezumi Cinnamon/Nagoya (NC/Nga) atopic mice with early dermatitis were transfected with pCpG-Mu $\gamma$  by a hydrodynamic tail vein injection at a dose of 0.05 or 0.2 pmol per mouse. The skin lesions improved only in mice receiving the high dose of pCpG-Mu $\gamma$ . IFN- $\gamma$  gene transfer resulted in a high mRNA expression of IFN- $\gamma$  and interleukin (IL)-12 and regulatory T cell (Treg) related cytokines, such as IL-10 and transforming growth factor- $\beta$ , in the spleen, whereas it reduced the IL-4 mRNA expression, and serum levels of immunoglobulin (Ig) G1 and IgE. In addition, the gene transfer markedly inhibited the epidermal thickening, infiltration of inflammatory cells into the skin, the occurrence of dry skin and pruritus. No exacerbating effect on the Th1-mediated contact dermatitis was observed after IFN- $\gamma$  gene transfer. Taken together, these results indicate that sustained IFN- $\gamma$  gene transfer induced polarized Th1 immunity under Th2-dominant conditions in NC/Nga mice, leading to an improvement in the symptoms of acute atopic dermatitis without adverse side effects.

*Gene Therapy* advance online publication, 23 August 2012; doi:10.1038/gt.2012.69

**Keywords:** atopic dermatitis; interferon- $\gamma$ ; NC/Nga mice; nonviral vector

## INTRODUCTION

Atopic dermatitis is a chronic inflammatory skin disorder accompanied by particular skin lesions. The main characteristics of atopic dermatitis are eczematous skin lesions, epidermal hypertrophy, intense pruritus and infiltration by inflammatory cells. Increased serum immunoglobulin (Ig) E and an excessive production of T helper 2 (Th2) cytokines are also frequently observed in patients with atopic dermatitis. The balance of Th1 and Th2 immune responses, which is maintained by their immunoregulatory cytokines under healthy conditions, is considered to be upset in atopic dermatitis. Generally, atopic dermatitis was classified into two phases, acute and chronic. In the acute phase of atopic dermatitis, patients often have raised Th2 cytokines, such as interleukin (IL)-4, IL-5 and IL-13, which induce the class switching of B cells to IgE secretion, but low levels of IFN- $\gamma$  or IL-12. In contrast, Th1 cytokines, especially IFN- $\gamma$ , are dominant in chronic phase of atopic dermatitis.<sup>1–6</sup> Therefore, the administration of interferon (IFN)- $\gamma$ , a typical Th1 cytokine that shifts the differentiation of naive T cells to the Th1 subtype and suppresses the production of Th2 cytokines, appears to be an attractive option for the treatment of acute phase of atopic dermatitis.<sup>7,8</sup>

It has recently been shown that regulatory T cells (Tregs), a subset of T cells, are involved in the modulation of allergic diseases. For example, Tregs and their related cytokines, IL-10 and transforming growth factor (TGF)- $\beta$ , have been reported to suppress Th2 responses and IgE production.<sup>9–11</sup> Furthermore, IFN- $\gamma$  as well as the IL-12-specific receptor subunit  $\beta$ 2 has important roles in the production of Tregs.<sup>12,13</sup>

Nishiki-nezumi Cinnamon/Nagoya (NC/Nga) mice is a mouse model of human atopic dermatitis. These mice spontaneously develop atopic dermatitis-like skin lesions around the age of 6–8 weeks when raised under conventional conditions but not in specific pathogen-free conditions. The skin lesions of conventional NC/Nga mice are characterized by erythema, hemorrhage, edema, erosion, scaling and dryness of the skin. Hyperproduction of IgE and Th2-type chemokines have also been reported in these mice. These clinical features are similar to those of human atopic dermatitis.<sup>14–17</sup>

We demonstrated in a previous study<sup>18</sup> that sustained expression of IFN- $\gamma$  is effective in preventing the onset of symptoms of atopic dermatitis in NC/Nga mice. The severity of the atopic lesions and other notable symptoms, such as scratching, dry skin, epidermal thickening, infiltration of inflammatory cells and the raised expression of Th2 cytokines and IgE, were markedly inhibited in mice receiving pCpG-Mu $\gamma$ , a plasmid expressing murine IFN- $\gamma$  for a long period of time.<sup>18</sup> To use IFN- $\gamma$  gene transfer in the treatment of atopic dermatitis patients, it is important to show that such gene transfer is effective not only in preventing the onset of the disease but also in improving the symptoms. IFN- $\gamma$  gene transfer could counteract the progression of atopic dermatitis through the induction of Treg cells.

In this study, we investigated whether IFN- $\gamma$  gene transfer was able to effectively treat dermatitis induced in NC/Nga mice. To do this, we evaluated the serum levels of IgE and IgG1, the mRNA expression of Th1 and Treg cytokines, transepidermal water loss (TEWL), the number of scratching episodes, the epidermal

<sup>1</sup>Department of Biopharmaceutics and Drug Metabolism, Graduate School of Pharmaceutical Sciences, Kyoto University, Kyoto, Japan; <sup>2</sup>Department of Dermatology, Graduate School of Medicine, Kyoto University, Kyoto, Japan and <sup>3</sup>Department of Pharmacotherapeutics, Faculty of Pharmaceutical Sciences, Doshisha Women's College of Liberal Arts, Kyoto, Japan. Correspondence: Dr M Nishikawa, Department of Biopharmaceutics and Drug Metabolism, Graduate School of Pharmaceutical Sciences, Kyoto University, 46-29 Yoshidashimoadachi-cho, Sakyo-ku, Kyoto 606-8501, Japan.

E-mail: makiya@pharm.kyoto-u.ac.jp

Received 22 March 2012; revised 20 July 2012; accepted 30 July 2012



thickening and the infiltration of inflammatory cells into the skin. In addition, the effect of sustained IFN- $\gamma$  gene transfer on contact dermatitis was also examined to assess the safety of the gene transfer process.

## RESULTS

Time-course and pharmacokinetic parameters of IFN- $\gamma$  after hydrodynamic injection of pCpG-Mu $\gamma$

Figure 1 shows the time-course of the concentrations of IFN- $\gamma$  in the serum after hydrodynamic injection of pCpG-Mu $\gamma$ . The serum levels of IFN- $\gamma$  were dependent on the plasmid dose, and the higher dose of 0.2 pmol resulted in significantly higher concentrations for the first 4 days compared with the lower dose. The profiles were analyzed to obtain area under the concentration-time curve and mean residence time values. Table 1 summarizes the C<sub>max</sub>, area under the concentration-time curve and mean residence time after IFN- $\gamma$  gene transfer. The C<sub>max</sub> and area under the concentration-time curve were increased by increasing the plasmid dose, whereas the mean residence time was hardly affected by the dose.

Effects of IFN- $\gamma$  gene transfer on the skin lesions of NC/Nga mice NC/Nga mice at the age of 7–8 weeks, which already developed atopic dermatitis-like symptoms, were used to assess the severity of skin lesions. Figure 2 shows the time-course of the clinical skin score of NC/Nga mice after injection of pCpG-Mu $\gamma$ . The score of mice treated with the lower dose pCpG-Mu $\gamma$  increased with time and was not significantly different from that of the untreated mice for the first 2 weeks after gene transfer. These results contradicted those of our previous study, in which the lower dose of pCpG-Mu $\gamma$  (0.05 pmol per mouse) was effective in preventing the onset of atopic dermatitis.<sup>18</sup> In contrast, the clinical skin score of mice receiving 0.2 pmol pCpG-Mu $\gamma$  was significantly lower than those of the other two groups over the 5-week observation period. Based on these findings, the dose of the plasmid was set at 0.2 pmol per mouse in the subsequent experiments to study the therapeutic effects of pCpG-Mu $\gamma$  in NC/Nga mice with dermatitis. To confirm the effects of IFN- $\gamma$ , a control plasmid pCpG-mcs (Invivogen, San Diego, CA, USA) was administered to NC/Nga mice. However, the clinical skin score was hardly affected by this treatment (data not shown).

Serum concentrations of IgG1 and IgE in NC/Nga mice after IFN- $\gamma$  gene transfer

Figure 3 shows the time-course of the concentration of IgG1 (Figure 3a) and IgE (Figure 3b) in the serum of NC/Nga mice after injection of pCpG-Mu $\gamma$ . Both the serum levels of IgG1 and IgE of the pCpG-Mu $\gamma$ -treated mice were significantly lower than those of the untreated mice at several time points, suggesting that the production of these Th2-mediated Igs in NC/Nga mice was at least partly inhibited by IFN- $\gamma$  gene transfer.

mRNA expression of Th1, Th2 and Treg cytokines in the spleen of NC/Nga mice after IFN- $\gamma$  gene transfer

The high concentrations of IFN- $\gamma$  in the serum were expected to induce the changes in the immunological status of NC/Nga mice. Therefore, the spleen, a major lymphoid organ, was excised and the mRNA expression of IFN- $\gamma$ , IL-12, IL-4, IL-10 and TGF- $\beta$  was measured. Figure 4 shows the x-fold increase in mRNA expression by pCpG-Mu $\gamma$ -treated mice compared with untreated mice. The mRNA expression of IFN- $\gamma$  and IL-12 in the pCpG-Mu $\gamma$ -treated mice was, respectively, 3- and 1.7-fold higher than that in the untreated mice. In addition, the mRNA expression of IL-10 and TGF- $\beta$  was also significantly higher in the pCpG-Mu $\gamma$ -treated group. On the other hand, the mRNA expression of IL-4, a Th2 cytokine, was reduced to about half in the pCpG-Mu $\gamma$ -treated mice.

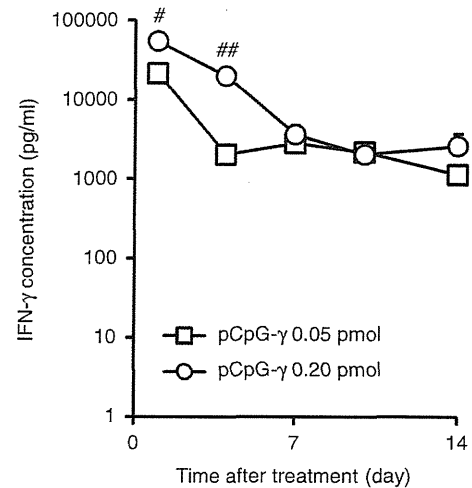


**Figure 1.** Time-course of the concentration of IFN- $\gamma$  in serum of NC/Nga mice after hydrodynamic injection of 0.05 or 0.2 pmol pCpG-Mu $\gamma$ . The results are expressed as the mean  $\pm$  s.e.m. of five mice. #, ## $P$  < 0.05, 0.01, compared with the lower dose group.

**Table 1.** C<sub>max</sub>, AUC and MRT of serum IFN- $\gamma$  after hydrodynamic injection of pCpG-Mu $\gamma$  into mice

Dose (pmol per mouse)	C <sub>max</sub> (ng ml <sup>-1</sup> )	AUC (ng day ml <sup>-1</sup> )	MRT (day)
0.05	21.3 $\pm$ 1.5	71.3 $\pm$ 7.9	4.67 $\pm$ 0.78
0.2	54.0 $\pm$ 10 <sup>a</sup>	204 $\pm$ 35 <sup>b</sup>	4.21 $\pm$ 0.70

Abbreviations: AUC, area under the concentration-time curve; IFN, interferon; MRT, mean residence time. The C<sub>max</sub> values were obtained at 1 day after hydrodynamic injection of pCpG-Mu $\gamma$ , and are expressed as the mean  $\pm$  s.e.m. of five mice. The AUC and MRT were calculated by moment analysis, and are expressed as the calculated mean  $\pm$  s.e.m. of five mice. <sup>a</sup> $P$  < 0.05, compared with the lower dose (0.05 pmol per mouse) group. <sup>b</sup> $P$  < 0.01, compared with the lower dose (0.05 pmol per mouse) group.

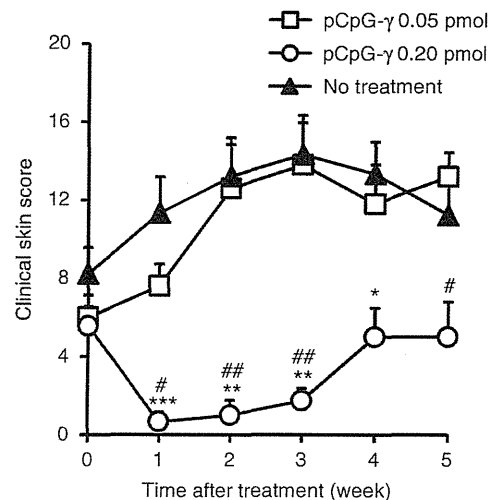


**Figure 2.** Time-course of the clinical skin score of NC/Nga mice after hydrodynamic injection of pCpG-Mu $\gamma$ . The results are expressed as the mean  $\pm$  s.e.m. of five (0.05 pmol and 0.2 pmol pCpG-Mu $\gamma$ -treated groups) and nine mice (the untreated group). \*, \*\*, \*\*\* $P$  < 0.05, 0.01, 0.001, compared with the untreated group; #, ## $P$  < 0.05, 0.01, compared with the lower dose group.

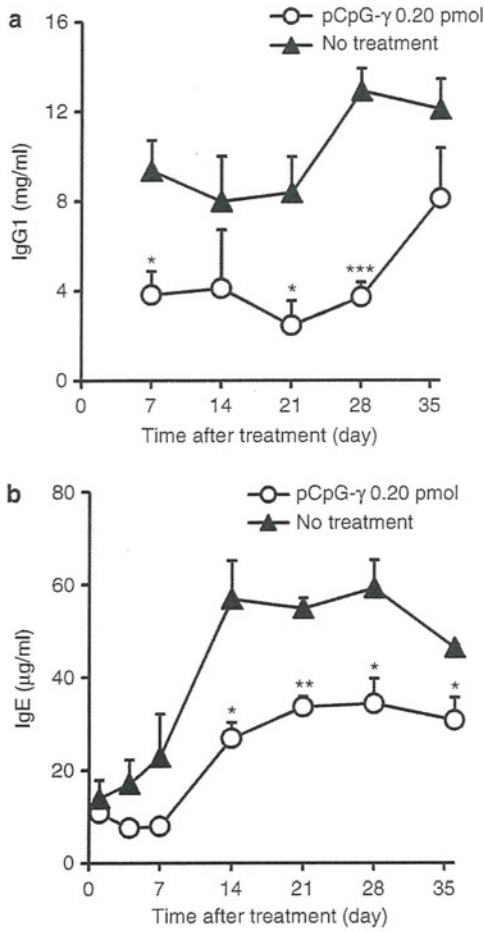


**Figure 3.** Time-course of the concentration of IgG1 (a) and IgE (b) in serum of NC/Nga mice after hydrodynamic injection of 0.05 or 0.2 pmol pCpG-Mu $\gamma$ . The results are expressed as the mean  $\pm$  s.e.m. of four mice. \* \*\* \*\*\* $P$ <0.05, 0.01, 0.001, compared with the untreated group.

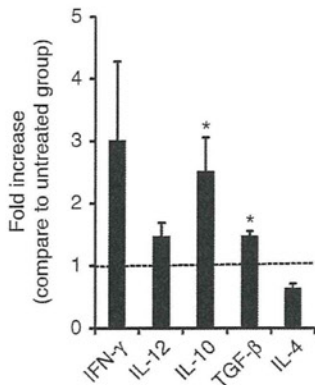


**Figure 4.** mRNA expression of cytokines in spleen cells of NC/Nga mice. Spleens of untreated mice and pCpG-Mu $\gamma$ -treated mice were excised at day 36 after treatment. mRNA expression was normalized with that of glyceraldehyde 3-phosphate dehydrogenase (GAPDH). The results are expressed as the mean  $\pm$  s.e.m. of three (pCpG-Mu $\gamma$ -treated group) or four mice (the untreated group). \* $P$ <0.05 compared with the untreated group.

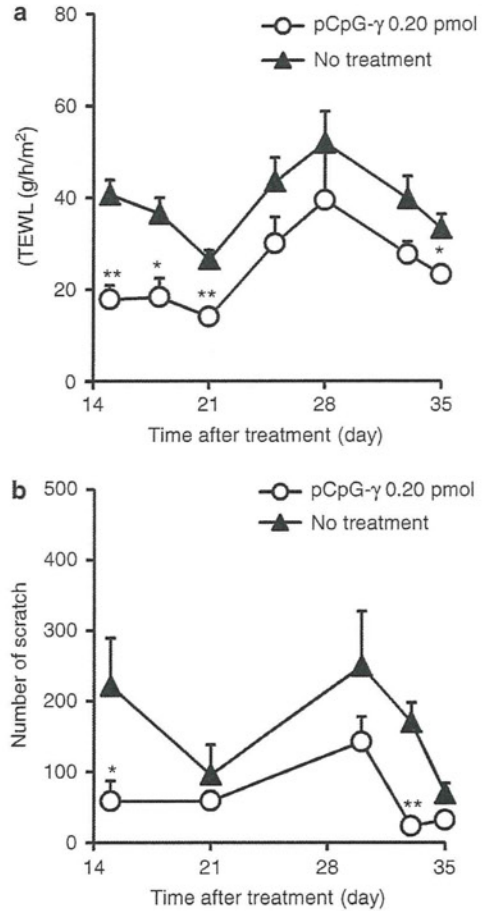


**Figure 5.** Time-course of the TEWL of the dorsal skin (a) and number of scratching episodes (b) of NC/Nga mice untreated or after hydrodynamic injection of 0.2 pmol pCpG-Mu $\gamma$ . The results are expressed as the mean  $\pm$  s.e.m. of four mice. \* \*\* $P$ <0.05, 0.01, compared with the untreated group.

TEWL and scratching behavior of NC/Nga mice after IFN- $\gamma$  gene transfer

To evaluate the severity of skin dryness and itchiness, the TEWL<sup>19</sup> and the number of scratching episodes were measured. Figure 5a shows the time-course of the TEWL of NC/Nga mice from day 15 to day 35 after injection of pCpG-Mu $\gamma$ . The TEWL value of the pCpG-Mu $\gamma$ -treated mice was significantly lower than that of the untreated mice on days 15, 18, 21 and 35 after gene transfer. Figure 5b shows the number of scratching episodes during a 30-min period of observation. The number of scratching episodes exhibited by the mice receiving pCpG-Mu $\gamma$  was fewer than that of the untreated mice at all-time points examined and the difference was significant on days 15 and 33 after injection of pCpG-Mu $\gamma$ . These results indicate that IFN- $\gamma$  gene transfer relieves the pruritus, a common symptom of atopic dermatitis that may lead to destruction of the skin barrier and is related to the increased TEWL of NC/Nga mice.<sup>20,21</sup>

Histopathological examination of skin sections of NC/Nga mice  
Figure 6 shows the hematoxylin and eosin sections (Figures 6a and b) and toluidine blue-stained sections (Figures 6c and d) of the dorsal skin of NC/Nga mice at 36 days after treatment. The sections of the untreated mice showed obvious thickening of the epidermis (Figures 6a and c). However, these characteristic



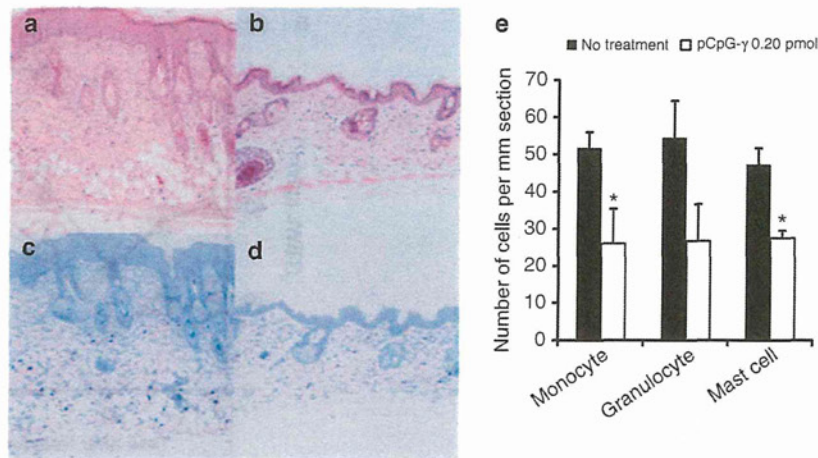


**Figure 6.** Hematoxylin and eosin (H&E) (a, b) and toluidine blue (c, d) sections of the dorsal skin of NC/Nga mice untreated (a, c) or pCpG-Mu $\gamma$ -treated (b, d). Numbers of inflammatory cells in skin sections (e). The numbers of cells were expressed as the mean  $\pm$  s.e.m. of three (pCpG-Mu $\gamma$ -treated group) or four mice (the untreated group). \* $P < 0.05$  compared with the untreated group.

features of skin inflammation were hardly seen in the sections from the pCpG-Mu $\gamma$ -treated mice (Figures 6b and d). Furthermore, the numbers of monocytes, granulocytes and mast cells in the skin sections were counted (Figure 6e). The numbers of these cells infiltrating into the skin of the pCpG-Mu $\gamma$ -treated animals were about a half those in the untreated mice, and there were significant differences between the groups with regard to the number of monocytes and mast cells.

**Effect of IFN- $\gamma$  gene transfer on body temperature and liver injury**  
The body temperature of the mice was measured to monitor the side effects of the high-dose pCpG-Mu $\gamma$ . No significant difference was observed in body temperature between the treated and untreated groups (data not shown). In addition, there were no significant differences in the serum aspartate aminotransferase and alanine aminotransferase levels between the pCpG-Mu $\gamma$ -treated and the untreated groups (data not shown).

**Effect of IFN- $\gamma$  gene transfer on contact dermatitis**

There are some concerns that IFN- $\gamma$  gene transfer might increase the risk of Th1-associated diseases. To clarify this issue, the ear swelling response in the oxazolone (OX)-induced contact dermatitis model was used to evaluate the contact hypersensitivity response in mice. As shown in Figure 7, OX treatment induced ear swelling but this response was not exacerbated by IFN- $\gamma$  gene transfer.

## DISCUSSION

NC/Nga mice spontaneously develop atopic dermatitis-like skin lesions around the age of 6–8 weeks when raised under conventional condition. After that, the severity of the skin lesions and the parameters reflecting the severity, such as serum IgE level, increases with age. A previous study reported that the serum IgE levels of conventional NC/Nga mice increased markedly from 6 weeks of age to around 10 weeks and reached plateau at 17 weeks.<sup>16</sup> Thus, the mice with atopic dermatitis at the age of 7–8 weeks, which were used in this study, represent a suitable model to evaluate the therapeutic effect of IFN- $\gamma$  in the acute phase of atopic dermatitis. In this study, we demonstrated that pCpG-Mu $\gamma$  is effective not only in preventing the onset of this condition but also in alleviating the symptoms of the disease, although a higher dose of pCpG-Mu $\gamma$  was required to treat the symptoms of NC/Nga

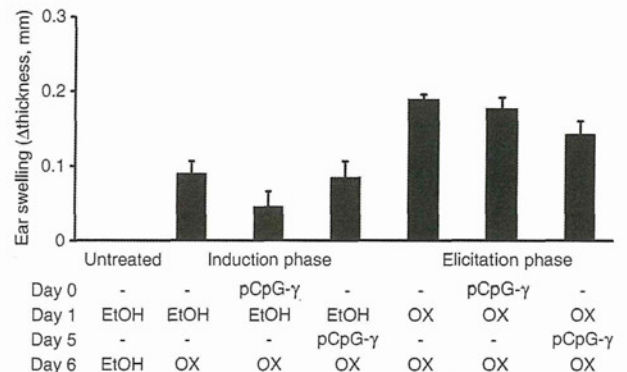


**Figure 7.** Ear swelling response in OX-treated mice. pCpG-Mu $\gamma$  was injected on day 0 or day 5. Mice were sensitized by OX or ethanol on the shaved abdomen on day 1 and on the right ear on day 6. Ear thickness was measured 24 h after the last OX application. Data are expressed as the mean  $\pm$  s.e.m. of four mice.

mice with dermatitis. The mRNA expression of IFN- $\gamma$  and IL-12, Th1 cytokines, in the spleen of mice receiving pCpG-Mu $\gamma$  was increased and accompanied with a reduced expression of IL-4 mRNA in the spleen and reduced levels of serum IgG1 and IgE (Figure 3). IFN- $\gamma$  acts in conjunction with IL-12 by mediating a positive feedback loop to drive the Th1 response and inhibits IL-4 production by Th2 cells, resulting in the suppression of IgE and IgG1 secretion by B cells.<sup>22–24</sup> The mRNA expression of IL-10 and TGF- $\beta$ , two representative Treg cytokines, in the spleen of mice receiving pCpG-Mu $\gamma$  were also increased. It has been reported that Tregs inhibit Th2 cell function in allergic diseases by releasing IL-10 and TGF- $\beta$ .<sup>11,25</sup> The development of atopic dermatitis-like skin lesions in NC/Nga mice was suppressed by IL-10 expressing plasmid DNA.<sup>26</sup> It is possible that the increased expression of IFN- $\gamma$  and IL-12 might induce Treg differentiation<sup>12,13</sup> and partially contributed to these immunological changes by suppressing Th2 cell response. Taking all these findings into consideration, it is likely that IFN- $\gamma$  gene transfer stimulates IL-12 production and these two Th1 cytokines act synergistically to polarize the T-cell response toward Th1 subset and inhibit IgG1 and IgE production by suppressing the Th2 pathway. Further investigation is needed

to prove whether the induction of Treg cytokines is related to these changes.

Scratching destroys skin barriers and worsens skin lesions,<sup>20,21</sup> which is closely linked to an increased TEWL. Histological examination of the skin sections clearly showed that IFN- $\gamma$  gene transfer markedly suppressed skin inflammation and the infiltration of monocytes, granulocytes and mast cells. Mast cells can be sensitized by IgE and regulate the secretion of cytokines, such as IL-4, which subsequently mediates the recruitment of leukocytes,<sup>27</sup> so that the reduced infiltration of these inflammatory cells into the skin could be due to the reduced production of IgE and IL-4. This suppression will prevent mice from scratching, which will accelerate skin repair and reduce TEWL. The number of scratching episodes of mice receiving pCpG-Mu $\gamma$  was lower than that of the untreated mice at all-time points, although it was fluctuated in the both groups. This could be explained by the difference in the time for measurement in each day,<sup>28</sup> which was not be controlled in this study.

The use of IFN- $\gamma$  as a therapeutic agent would be a double-edged sword. The need for a high dose of 0.2 pmol per mouse to treat, not to prevent, atopic dermatitis symptoms increases the chance of adverse reactions. The most common adverse events of IFN- $\gamma$  therapy, which have been evidenced in several clinical trials, are 'flu-like' symptoms, including fever, headache, fatigue and myalgia. Diarrhea, erythema at the injection site and the elevation of liver transaminase levels have also been reported in patients receiving the therapy. These common adverse events are generally transient and well tolerated.<sup>29–34</sup> In this study, we measured the body temperature and the liver transaminase levels in serum of mice for monitoring the signs of adverse events and demonstrated that IFN- $\gamma$  gene transfer is safe for use in mice as long as the dose of the plasmid is 0.2 pmol per mouse or lower. However, the clinical skin score seems to return to baseline level at 4 weeks after treatment with this dose of plasmid (Figure 2). This result may be explained by the reduction of IFN- $\gamma$  levels in the serum of mice with time, thus increasing the dose of pCpG-Mu $\gamma$  within the safety range could be an option to extend the duration of therapeutic effects. Recently, we have established a plasmid DNA expressing IFN $\gamma$  in a constant manner with no initial high concentration of IFN- $\gamma$  that could cause the unwanted effects.<sup>35</sup> This novel IFN- $\gamma$  expressing plasmid would also be useful to enhance the therapeutic effect of IFN- $\gamma$ . Another interesting point is that IFN- $\gamma$  has been reported to be dominant in the skin of patients with chronic atopic dermatitis.<sup>5</sup> Further investigation is required to prove whether IFN- $\gamma$  gene transfer is suitable for the treatment of chronic phase of atopic dermatitis.

In conclusion, we have demonstrated that sustained transgene expression of IFN- $\gamma$  is effective in treating the atopic dermatitis in NC/Nga mice without any apparent adverse effects. These results raise a possibility that IFN- $\gamma$  gene transfer can be a therapeutic option for patients with acute-phase atopic dermatitis.

## MATERIALS AND METHODS

### Animals

In all, 7- to 8-week-old male NC/Nga mice and 7-week-old female C57BL/6 mice were purchased from Japan SLC, Inc. (Shizuoka, Japan). The mice were raised and maintained on a standard food and water diet under conventional housing conditions. The NC/Nga group spontaneously developing dermatitis was used as a model of atopic dermatitis. The protocol for the animal experiments was approved by the Animal Experimentation Committee of the Graduate School of Pharmaceutical Sciences of Kyoto University.

### *In vivo* gene transfer of IFN- $\gamma$

The plasmid pCpG-Mu $\gamma$  constructed previously<sup>36</sup> was used for the treatment. The naked plasmid pCpG-Mu $\gamma$  was dissolved in normal saline

solution and injected into the tail vein of the mice by the hydrodynamic injection method<sup>37,38</sup> at a dose of 0.05 or 0.2 pmol per mouse on day 0.

### Measurement of the concentrations of IFN- $\gamma$ , IgG1 and IgE

Blood samples were obtained from the tail vein at indicated times after gene transfer, kept at 4 °C for 2 h to allow clotting, and then centrifuged to obtain serum. The concentration of IFN- $\gamma$ , IgG1 and IgE in the serum was measured using ELISA kits (Ready-SET-Go! Mouse IFN- $\gamma$  ELISA, eBioscience, San Diego, CA, USA; Mouse IgG1 ELISA Quantitation Set, Bethyl Laboratories, Inc., Montgomery, TX, USA; and Mouse IgE ELISA Set, BD Biosciences, San Diego, CA, USA) according to the manufacturer's instructions.

### Calculation of the pharmacokinetics parameters of IFN- $\gamma$ gene transfer

The area under the concentration-time curve and the mean residence time of IFN- $\gamma$  after gene transfer were calculated from the concentrations of IFN- $\gamma$  in the serum of NC/Nga mice using moment analysis.<sup>39</sup>

### Real-time PCR analysis of cytokine expression

RNA was extracted from approximately 100 mg of spleen samples using Sepasol RNA I Super (Nacalai Tesque, Kyoto, Japan). A mixture of recombinant DNase I-RNase-free (TAKARA, Shiga, Japan) and RNase OUT recombinant ribonuclease inhibitor (Invitrogen, Carlsbad, CA, USA) was used for DNase treatment. Reverse transcription was performed using a ReverTra Ace qPCR RT Kit (TOYOBO, Osaka, Japan). For a quantitative analysis of mRNA expression, reverse transcribed samples were amplified by PCR using the primers listed below, and a LightCycler FastStart DNA Master<sup>PLUS</sup> SYBR Green I kit (Roche Diagnostics GmbH, Mannheim, Germany) in a LightCycler instrument (Roche Diagnostics GmbH) according to the manufacturer's protocols. The sequences of primers used were as follows (forward and reverse, respectively): IFN- $\gamma$  (5'-ATGAACGCTACACA CTGCATC-3' and 5'-CCATCCTTTTGCCAGTTCCTC-3'), IL-12 (5'-CATCGATGAG CTGATGCAGT-3' and 5'-CAGATAGCCCATCACCTGT-3'), IL-4 (5'-ACAGGAG AAGGGACGCCAT-3' and 5'-GAAGCCCTACAGACGAGCTCA-3'), IL-10 (5'-CCA AGCCTTATCGGAAATGA-3' and 5'-TTTTCACAGGGGAGAAATCG-3'), TGF- $\beta$  (5'-TTGCTTCAGCTCCACAGAGA-3' and 5'-TGGTGTAGAGGGCAAGGAC-3') and glyceraldehyde 3-phosphate dehydrogenase (5'-CTGCCAAGTATGATG ACATCAAGAA-3' and 5'-ACCAGGAAATGAGCTTGACA-3'). Individual PCR products were analyzed by melting curve analysis and the length of the products was determined by agarose gel electrophoresis. The mRNA expression of each gene was normalized using the mRNA level of glyceraldehyde 3-phosphate dehydrogenase.

### Scoring skin lesions

Skin lesions were scored at indicated times after gene transfer according to the criteria previously reported.<sup>18</sup> In brief, the scoring was based on (i) the eczema severity, (ii) erosion/excoriation, (iii) scale formation, (iv) erythema/hemorrhage, (v) inflammation of the face and (vi) inflammation of the ear. The total clinical skin severity score was defined as the sum of the each of the six signs (none = 0; mild = 1; moderate = 2; and severe = 3).

### Measurement of TEWL

TEWL was measured using an evaporimeter (VAPO SCAN, AS-VT 100RS, Asahi Biomed, Yokohama, Japan) applied to the shaved back of the mice.

### Observation of scratching behavior

The scratching behavior was recorded on video for 30 min on days 15 and 21. The videotape was played back at a later time and the number of scratching episodes was counted manually. A series of scratching behaviors, starting with the stretching of the hind paws to the head, face or back and ending with the set-back of the paws, were counted as one bout of scratching. On days 30, 33 and 35 after gene transfer, the scratching behavior was monitored using a SCLABA Real (Noveltec Inc., Kobe, Japan), an automated system to analyze the scratching behavior of small animals. Each mouse was put into an acrylic cage, and its behavior was recorded for 30 min. The number of scratching episodes was automatically quantified.<sup>18</sup>



### Analysis of skin sections

The dorsal skin of the mice was excised, fixed in 4% paraformaldehyde and embedded in paraffin. Then, 4- $\mu$ m-sections were obtained using a microtome and stained with hematoxylin and eosin for histological evaluation and quantification of the numbers of monocytes and granulocytes or with toluidine blue for the detection of mast cells. The number of monocytes, granulocytes and mast cells were manually counted under a microscope, and expressed as the number per unit length of the skin section.

### Monitoring of adverse effects of IFN- $\gamma$ gene transfer

The body temperature of the mice was monitored using a digital rectal thermometer (Physitemp Instruments Inc., Clifton, NJ, USA). To assess liver damage, the serum alanine aminotransferase and aspartate aminotransferase levels of the mice were assayed using commercial test reagents (Transaminase CII-Test Wako, Wako Pure Chemical Industries, Osaka, Japan).

### OX-induced contact hypersensitivity

The plasmid pCpG-Mu $\gamma$  was injected into the tail vein of C57BL/6 mice (female, 7-week-old) by the hydrodynamic injection method at a dose of 0.2 pmol per mouse on day 0 or day 5. Mice were sensitized by the application of 100  $\mu$ l 2% OX in ethanol (elicitation phase group) or ethanol alone (induction phase-group) to the shaved abdominal skin on day 1, followed by an application of 10  $\mu$ l 1% OX to the right ear on day 6. Ethanol was applied to the left ear. For the untreated group, ethanol was applied instead of OX to the abdomen and right ear on either day 1 or 6. At 24 h after the second application, the thickness of both ears was measured using a digital thickness gauge (Quick Mini, Mitutoyo Co., Kawasaki, Japan). Ear swelling was calculated from the difference in ear thickness between the hapten- and vehicle-treated ears.

### Statistical analysis

Statistical significance was evaluated by analysis of variance with a *post-hoc* Tukey–Kramer test for multiple comparisons (clinical skin scores) and Student's *t*-test for comparisons between two given groups. The level of statistical significance was set at  $P < 0.05$ .

### ABBREVIATIONS

IFN- $\gamma$ , interferon  $\gamma$ ; Ig, immunoglobulin; IL, interleukin; Th, T helper.

### CONFLICT OF INTEREST

The authors declare no conflict of interest.

### ACKNOWLEDGEMENTS

This work was supported in part by a Grant-in-aid for Scientific Research (B) from the Japan Society for the Promotion of Science (JSPS).

### REFERENCES

- Oyoshi MK, He R, Kumar L, Yoon J, Geha RS. Cellular and molecular mechanisms in atopic dermatitis. *Adv Immunol* 2009; **102**: 135–226.
- Bieber T. Atopic dermatitis. *N Engl J Med* 2008; **358**: 1483–1494.
- Homey B, Steinhoff M, Ruzicka T, Leung DYM. Cytokines and chemokines orchestrate atopic skin inflammation. *J Allergy Clin Immunol* 2006; **118**: 178–189.
- Boguniewicz M, Leung DYM. Atopic dermatitis. *J Allergy Clin Immunol* 2006; **117**: S475–S480.
- Rebane A, Zimmermann M, Aab A, Baurecht H, Koreck A, Karelson M *et al*. Mechanisms of IFN- $\gamma$ -induced apoptosis of human skin keratinocytes in patients with atopic dermatitis. *J Allergy Clin Immunol* 2012; **129**: 1297–1306.
- Salem SAM, Diab HM, Fathy G, Obia LM, Sayed SBE. Value of interleukins 4, 10, 12, 18 and Interferon gamma in acute versus chronic atopic dermatitis. *J Egypt Women Dermatol Soc* 2010; **7**: 56–60.
- Chang TT, Stevens SR. Atopic dermatitis: the role of recombinant interferon- $\gamma$  therapy. *Am J Clin Dermatol* 2002; **3**: 175–183.
- Akhavan A, Rudikoff D. Atopic dermatitis: systemic immunosuppressive therapy. *Semin Cutan Med Surg* 2008; **27**: 151–155.

- Akdis M, Blaser K, Akdis CA. T regulatory cells in allergy: novel concepts in the pathogenesis, prevention, and treatment of allergic diseases. *J Allergy Clin Immunol* 2005; **116**: 961–968.
- Ozdemir C, Akdis M, Akdis CA. T regulatory cells and their counterparts: masters of immune regulation. *Clin Exp Allergy* 2009; **39**: 626–639.
- Larche M. Regulatory T cells in allergy and asthma. *CHEST* 2007; **132**: 1007–1014.
- Zhao Z, Yu S, Fitzgerald DC, Elbehi M, Ciric B, Rostami AM *et al*. IL-12R $\beta$ 2 promotes the development of CD4<sup>+</sup>CD25<sup>+</sup> regulatory T cells. *J Immunol* 2008; **181**: 3870–3876.
- Wang Z, Hong J, Sun W, Xu G, Li N, Chen X *et al*. Role of IFN- $\gamma$  in induction of Foxp3 and conversion of CD4<sup>+</sup>CD25<sup>+</sup> T cells to CD4<sup>+</sup> Tregs. *J Clin Invest* 2006; **116**: 2434–2441.
- Jin H, He R, Oyoshi M, Geha RS. Animal models of atopic dermatitis. *J Invest Dermatol* 2009; **129**: 31–40.
- Matsuda H, Watanabe N, Geba GP, Sperl J, Tszdzuki M, Hiroi J *et al*. Development of atopic dermatitis-like skin lesion with IgE hyperproduction in NC/Nga mice. *Int Immunol* 1997; **9**: 461–466.
- Suto H, Matsuda H, Mitsuishi K, Hira K, Uchida T, Unno T *et al*. NC/Nga mice: a mouse model for atopic dermatitis. *Int Arch Allergy Immunol* 1999; **120**(suppl 1): 70–75.
- Vestergaard C, Yoneyama H, Murai M, Nakamura K, Tamaki K, Terashima Y *et al*. Overproduction of Th2-specific chemokines in NC/Nga mice exhibiting atopic dermatitis-like lesions. *J Clin Invest* 1999; **104**: 1097–1105.
- Hattori K, Nishikawa M, Watcharanurak K, Ikoma A, Kabashima K, Toyota H *et al*. Sustained exogenous expression of therapeutic levels of IFN- $\gamma$  ameliorates atopic dermatitis in NC/Nga mice via Th1 polarization. *J Immunol* 2010; **184**: 2729–2735.
- Simonsen L, Fullerton A. Development of an *in vitro* skin permeation model simulating atopic dermatitis skin for the evaluation of dermatological products. *Skin Pharmacol Physiol* 2007; **20**: 230–236.
- Yamamoto M, Haruna T, Ueda C, Asano Y, Takahashi H, Iduhara M *et al*. Contribution of itch-associated scratch behavior to the development of skin lesions in Dermatophagoides farinae-induced dermatitis model in NC/Nga mice. *Arch Dermatol Res* 2009; **301**: 739–746.
- Hashimoto Y, Arai I, Nakanishi Y, Sakurai T, Nakamura A, Nakaie S. Scratching of their skin by NC/Nga mice leads to development of dermatitis. *Life Sci* 2004; **76**: 783–794.
- Schroder K, Hertzog PJ, Ravasi T, Hume DA. Interferon- $\gamma$ : an overview of signals, mechanism and functions. *J Leukoc Biol* 2004; **75**: 163–189.
- Finkelman FD, Katona IM, Mosmann TR, Coffman RL. IFN- $\gamma$  regulates the isotypes of Ig secreted during *in vivo* humoral immune response. *J Immunol* 1988; **140**: 1022–1027.
- Nakagome K, Okunishi K, Imamura M, Harada H, Matsumoto T, Tanaka R *et al*. IFN- $\gamma$  attenuates antigen-induced overall immune response in the airway as a Th1-type immune regulatory cytokine. *J Immunol* 2009; **183**: 209–220.
- Palomares O, Yaman G, Azkur A, Akkoc T, Akdis M, Akdis CA. Role of Treg in immune regulation of allergic diseases. *Eur J Immunol* 2010; **40**: 1232–1240.
- Jung BG, Cho SJ, Ko JH, Lee BJ. Inhibitory effects of interleukin-10 plasmid DNA on the development of atopic dermatitis-like skin lesions in NC/Nga mice. *J Vet Sci* 2010; **11**: 213–220.
- Liu FT, Goodarzi H, IgE Chen HY. Mast cells, and eosinophils in atopic dermatitis. *Clinic Rev Allerg Immunol* 2011; **41**: 298–310.
- Takahashi N, Arai I, Honma Y, Hashimoto Y, Harada M, Futaki N *et al*. Scratching behavior in spontaneous- or allergic contact-induced dermatitis in NC/Nga mice. *Exp Dermatol* 2005; **14**: 830–837.
- Miller CHT, Maher SG, Young HA. Clinical use of interferon- $\gamma$ . *Ann NY Acad Sci* 2009; **1182**: 69–79.
- Tovey MG, Lallemand C. Safety, tolerability, and immunogenicity of interferons. *Pharmaceuticals* 2010; **3**: 1162–1186.
- Schneider LC, Baz Z, Zarcone C, Zurakowski D. Long-term therapy with recombinant interferon-gamma for atopic dermatitis. *Ann Allergy Asthma Immunol* 1998; **80**: 263–268.
- Jang I, Yang J, Lee H, Yi J, Kim H, Kim C *et al*. Clinical improvement and immunohistochemical findings in severe atopic dermatitis treated with interferon gamma. *J Am Acad Dermatol* 2000; **42**: 1033–1040.
- The International Chronic Granulomatous Disease Cooperative Study Group. A controlled trial of interferon gamma to prevent infection in chronic granulomatous disease. *N Engl J Med* 1991; **324**: 509–516.
- Stuart K, Levy DE, Anderson T, Axiotis CA, Dutcher JP, Eisenberg A *et al*. Phase II study of interferon gamma in malignant carcinoid tumors (E9292): a trial of the Eastern Cooperative Oncology Group. *Invest New Drugs* 2004; **22**: 75–81.
- Ando M, Takahashi Y, Nishikawa M, Watanabe Y, Takakura Y. Constant and steady transgene expression of interferon- $\gamma$  by optimization of plasmid construct for safe and effective interferon- $\gamma$  gene therapy. *J Gene Med* 2012; **14**: 288–295.

- 36 Mitsui M, Nishikawa M, Zang L, Ando M, Hattori K, Takahashi Y *et al*. Effect of the content of unmethylated CpG dinucleotides in plasmid DNA on the sustainability of transgene expression. *J Gene Med* 2009; **11**: 435–443.
- 37 Liu F, Song Y, Liu D. Hydrodynamics-based transfection in animals by systemic administration of plasmid DNA. *Gene Therapy* 1999; **6**: 1258–1266.
- 38 Kobayashi N, Nishikawa M, Takakura Y. The hydrodynamics-based procedure for controlling the pharmacokinetics of gene medicines at whole body, organ and cellular levels. *Adv Drug Deliv Rev* 2005; **57**: 713–731.
- 39 Yamaoka K, Nakagawa T, Uno T. Statistical moments in pharmacokinetics. *J Pharmacokinetic Biopharm* 1978; **6**: 547–558.